

USGS External Research Program Final Technical Report
Award #99HQGR0031

REVISING MOMENT-MAGNITUDE EARTHQUAKE
CATALOGS FOR USE IN GENERATING THE
NATIONAL SEISMIC HAZARD MAPS

Bradley B. Woods

URS Group, Inc.
566 El Dorado Street.
Pasadena, CA 91101

email: bradley_woods@urscorp.com
tel: (626) 449-7650 / fax: (626) 449-3536

November 27, 2002

REVISING MOMENT-MAGNITUDE EARTHQUAKE CATALOGS FOR
USE IN GENERATING THE NATIONAL SEISMIC HAZARD MAPS

Bradley B. Woods

URS Group, Inc.
566 El Dorado Street
Pasadena, CA 91101
bradley_woods@urscorp.com

ABSTRACT

This is the first of a two-part study to revise the earthquake catalogs used in the preparation of the National Seismic-Hazard Maps (NSHM) (Frankel *et al.*, 1996), used to quantify seismic hazards in the continental U.S (Frankel, 1995); in particular, we are obtaining direct estimates of seismic moment (M_0) or moment magnitude (M_w) for earthquakes in the digitally-instrumented portion (1988+) of these catalogs. The current catalogs for the western and central/eastern U.S. (WUS and CEUS, respectively) incorporate a variety of magnitude types, including m_b , M_L and M_s , converting them all to one magnitude scale -- M_w for WUS and $m_b Lg$ for CEUS, respectively. Further, the raw magnitudes are taken from a variety of sources. Thus catalog magnitudes are a heterogeneous lot. A consistent set of moment estimates for these events will lead to the generation of more accurate seismic hazard maps. Revising these catalogs with a consistent set of moment magnitudes (M_w 's) is the purpose of this work; in particular, this report details the results for revising the western U. S., *i. e.* the WUS catalog. For this purpose we have developed a variant coda magnitude (M_C) -- after trying several variations -- which yields accurate, relatively well-constrained estimates of M_w using time-domain coda measurements of regional short-period seismograms, given by:

$$M_{w(coda)} = \log_{10}(A_c) + a_0 + a_1 \cdot \log_{10}(\tau) + a_2 \cdot \tau + a_3 \cdot \Delta,$$

where τ is the coda duration (after origin time), A_c is the coda amplitude measured in the tail portion of the seismogram, and Δ is epicentral distance. This method, a modified version of Mayeda's (1993) $m_b(LgCoda)$ measurement, is adopted for its ready application to analog as well as digital data, and for its small inter-station variance in magnitude/moment estimates. Moment estimates for WUS catalog events were collected, where available from catalogs or source studies, in order to create master events with "ground truth" moment magnitudes -- that is, earthquakes with well-constrained seismic moment (M_0) estimates determined from waveform-inversion source studies -- with which to calibrate $M_{w(coda)}$ for each regional station used. These M_w 's were also compared directly to the current WUS catalog's

values *via* regression analysis in order to ascertain the accuracy and consistency of the present catalog's magnitudes. The coda magnitude measurement provides single-station M_w estimates with standard errors ranging between 0.04 and 0.17, with the network-averaged value being 0.11 (half that of the WUS catalog values), when regressed against the master-event M_w 's. Using this method, coda magnitudes were calculated from regional seismograms for 224 1988+ events from the WUS catalog, in order to provide a revised, more accurate set of M_w 's for generating the seismic hazard maps. In quality checking the results, 6, or 2.6 percent, of the events within the period analyzed (1988-1995) were found, by cross-referencing local network catalogs, to be significantly smaller, *i. e.* by a full magnitude unit or more, or appear, in fact, to be non-existent.

INTRODUCTION

The objective of this work is to revise moment-magnitudes in the WUS and CEUS catalogs (Mueller *et al.*, 1997), which are used to generate the National Seismic Hazard Maps (NSHM) produced by the USGS (Frankel, 1995), in order to update these same maps. The project specifically addresses an objective of Element (1) of the 1998 NEHRP External Research Announcement, Products for Earthquake Loss Reduction: "*Compile new and upgrade existing...moment-magnitude-based earthquake catalogs from regional network data to provide input information for seismic hazard maps*".

In generating the 1997 NSHM, Frankel (1995) demonstrated that seismic hazard calculations based quantitatively on seismicity catalog information (location, time, and magnitude) yield results similar to those of elaborate studies by teams of experts that integrate various seismic, geophysical, and geological data (EPRI/SOG, 1986). This simpler methodology also has the advantage of being based on objective, quantifiable criteria, *i. e.* the spatial and temporal distribution of earthquakes. In order to capitalize on the strength of this method, which is its statistical robustness based on empirical data, it is important to use as accurate and comprehensive a seismicity catalog as possible. Earthquake source level, quantified by some magnitude scale, is of primary importance for this, indicating the need for accurate and consistent magnitudes for events in the catalog.

Reliable source quantification for earthquake catalogs is important in synthesizing accurate probabilistic seismic hazard maps using this empirical approach. Seismic moment (M_0) is a particularly useful parameter for quantifying seismic sources, as it is a physical parameter derived from seismic source theory and yields a stable measure of the earthquake long-period source spectrum. M_0 , or its magnitude equivalent M_w , provides a more direct and physically based estimate of ground motion than do empirically-based magnitude scales, such as m_b . Unlike these magnitude scales, seismic moment is a physical parameter which is directly proportional to ground motion and quantifies the long-period source character of earthquakes, being derived from seismic source theory. M_w then can directly compare source sizes between earthquakes in different geophysical regimes and different geographical regions. Further, seismologically-based models for estimating strong ground motion use seismic moment to quantify the size of earthquakes.

For these reasons, there is a strong preference for using seismic moment to quantify earthquake

magnitudes for seismic hazard calculations. The primary reason that all magnitudes are still being converted to m_b (or $m_b(Lg)$) for the CEUS catalog is that it is a link to historical eastern North American earthquake catalogs and to current and past magnitude practice. However, it makes more sense, for the purpose of modeling ground motions, to use seismic moment, or moment magnitude, instead to quantify earthquake size.

The current catalogs used to generate the national seismic hazard maps (Mueller *et al.* (1997)) use a unified magnitude system by converting various types of magnitudes into $m_b(Lg)$, a regional measurement tied to teleseismic m_b , for the central and eastern U.S. (CEUS) catalog, and into M_w for the western U.S. (WUS) catalog. These conversions are based on very general relationships among the various magnitude scales, such as local or Richter magnitude (M_L), Lg-wave magnitude ($m_b(Lg)$), and coda (M_c) or coda duration magnitude (M_D) (see Mueller *et al.* (1997) for details). Thus the catalogs are heterogeneous in nature and the magnitude values themselves are sensitive to the magnitude conversion used; further very few actual M_w values are used at all in generating the catalogs.

There are several shortcomings to this procedure and the converted magnitudes so generated. First of all, the scaling relations used to convert from the various magnitude scales to seismic-moment magnitude have some uncertainty in them, which in turn introduces error into the converted magnitude values. Moreover, the relationships used are determined from observations of older, analog-data events. Moment estimates for such events were obtained using approximate methods of analyzing analog data, or by spectral-level moment estimates based on questionable assumptions about the source (*i. e.* stress-drop), rather than from more current standard waveform or spectral moment-tensor inversion methods. Direct measure of seismic moment from digital data analysis provides a more accurate estimate of the source excitation level, or long-period source spectrum, still; consequently it would be preferable to use more recently established scaling relations between M_w and other magnitudes, rather than the ones used for the current moment-magnitude catalogs, which were established in the early 80's, before the advent of appreciable digital seismic data.

Furthermore, the scaling relationships between such magnitude scales and M_w are not that well established and can vary by geographic region as well as by the network used to obtain the measurement. Further, the scaling relationships themselves vary in different magnitude ranges and can

saturate at higher magnitudes, the precise behavior of which is not well established, *i. e.* parameterized, thereby incorporating more error in any magnitude conversion, particularly for larger earthquakes.

More importantly still, we have found by analysis of empirical scaling relationships between M_w and other magnitude scales for large data sets that the magnitude conversion formulae currently used to generate the catalog have certain biases to them which adversely affect the consequent M_w estimates. This problem is highlighted by comparing the current M_w catalog values to direct moment estimates for the same events. Figure 1a is a map of North America indicating earthquakes from the CEUS and WUS catalog (1963+) for which M_0 already has been directly determined by various source studies which model and invert long-period waveforms; hence these moment estimates are considered to be quite accurate. Figure 1b and c are plots of the regression of these moments, in terms of M_w , vs. the values in the WUS and CEUS catalogs, respectively. For this purpose the CEUS catalog magnitude values, which are actually in terms m_{bLg} , directly correspond to M_w in for $M_w \geq 4$ events -- that is, they convert one to one via the defined relations of Mueller *et al.* (1997) used to generate the catalog composite magnitudes.

There is considerable scatter in these regression relationships -- particularly for the WUS events, with a standard error of estimate of 0.29 magnitude units -- and the slope of the M_w relationship is less than unity for both cases. This second result implies that the WUS and CEUS catalog underestimate the M_w of larger events and correspondingly overestimate the values of smaller events; it should be kept in mind, however, that these relationships are also poorly constrained, due to the scatter in the data, so the scaling relationship may still have a slope of unity. Whatever the case, it is clear that direct moment estimates need to be made for instrumented events in these two catalogs in order to establish the accuracy of the present catalog values, and, in all likelihood, to revise them with new, improved M_w estimates obtained in a consistent fashion, which is the purpose of this work.

Furthermore, there appears to be a systematic negative moment-magnitude bias in the WUS catalog, since the conversion between M_0 , M_L , and m_b are all one-to-one in the magnitude range 4-6.8 (Mueller *et al.*, 1997). This relationship holds approximately within a limited magnitude range for CEUS earthquakes (Herrmann and Nuttli, 1982), but in the WUS it has been demonstrated that there is an offset of approximately 0.4 units between M_L and m_b (Chung and Bernreuter, 1981; and Herrmann

and Nuttli, 1982). To confirm this we took the moment data of Thio and Kanamori (1995) for southern California earthquakes and regressed them directly vs. m_b and M_L . In their study they showed that the moments, when converted to M_w , correlate well and directly with M_L , *i. e.* ($M_w = M_L$), see Figure 2d, whereas there appears to be an offset in the M_w - m_b relationship, shown in Figure 2b, for which a given event's m_b is approximately 0.2 magnitude units less than its M_w . This appears to apply at all magnitudes. Here we are discussing the fixed-slope ($m = 1$) results. The free-slope, or regular linear regression, results are also shown. In this case the M_w - m_b relationship (Figure 2a) is relatively poorly constrained relative to the $M_w = M_L$ one (Figure 2c); even then the standard error of the estimate is still fairly large, being 0.13 magnitude units, but the curve is well constrained, with error bars on the curves being hard to discern from the regression line itself.

This offset between m_b and M_L for a given M_w -sized event was observed with other earthquake populations analyzed as well in the same fashion, including those from the Berkeley moment catalog, and events from studies by Zhu and Helmberger (1996), and Kanamori *et al.* (1993), and ranged between 0.19 and 0.27. Although not quite as large as the offset found in these other studies, it is on the same order and of the same sign. Such m_b -magnitude biases will certainly affect M_w estimates based upon m_b values. Direct moment estimates avoid such magnitude conversion problems.

Thus the current hazard catalogs need to be updated, with respect to M_w , by incorporating direct moment estimates rather than inferred values based on generalized empirical relationships between M_w and other magnitude scales; or, when that is not possible, by determining better inter-magnitude scaling relationships, based on regression analysis of more comprehensive data sets, to convert the original raw magnitudes of various types from which the NSHM catalogs were generated

First, seismic moment estimates determined from regional source studies were compiled for events in the WUS catalog, *i. e.* WUS; when available, multiple M_w estimates were averaged. Such information is available for a only limited number of historical analog-recorded (pre-WWSN) earthquakes, but considerably more events recorded by the WWSN (World-Wide Seismic Network). However, with the advent of readily available, broad-band, high-dynamic-range digital data (1988+), earthquakes large enough to produce long-period signals have come to be routinely analyzed by moment-tensor inversion of regional waveforms, *e. g.* Zhao and Helmberger (1994) or spectral data, *e. g.* Thio and Kanamori

(1995). This subset of events from the WUS catalog were then used as master events for calibrating the individual station effective attenuation parameters; in effect they are "ground-truth" (GT) estimates of M_w and this term is used to refer to such magnitudes throughout the text and figures.

Next, we directly measure M_w for available regional waveforms. Since we are dealing with analog as well as later digital data, we desire to use a time-domain measure readily applicable to either type of data. We also want a method useful for the entire range of magnitudes of interest, *i. e.* $3.5 < M_w < 7.5$. To directly obtain moment estimates for smaller events (generally $M_w < 4.5$), for which long-period waveform information generally is not available because of noise-level considerations, requires a method using information from short-period seismograms. To this end we employ a measurement of the seismic coda of the regional wave train to obtain estimates of seismic moment. Measuring short-period coda -- that is, within the bandwidth of a short-period WWSN instrument (WWSP) -- for this purpose has shown promise.

The relatively recent development of short-period coda and coda-duration magnitude scales (M_C and M_d , respectively), which yield reliable moment estimates even for smaller events ($M < 4$), can be used to provide M_w measurements for events which previously could previously only be quantified by local (M_L) or regional ($m_b Lg$ or mb_{P_n}) magnitude because of signal-to-noise measuring thresholds for longer-period waveform measurements necessary for M_s or conventional M_w estimates. As discussed previously, the scaling relationships between such local and regional magnitude scales and seismic moment, or M_w are not well established or constrained; thus direct estimates of seismic moment for such smaller events, using coda-wave measurements, is a significant improvement over extrapolating from some regional or local magnitude scale. Coda-based M_w measurements then are of particular use for revising the CEUS catalog, which includes events down to $m_b = 3.0$, for which conventional moment estimates are not obtainable.

Coda measurements have several other advantages:

- 1) Coda amplitudes vary little with geologic structure and show little or no effect of azimuthal source radiation effects, thus allowing accurate single-station measurements;
- 2) Path-corrected coda amplitudes can be measured consistently over a large region, which makes

comparison of source parameters for events throughout the U.S. possible, using a common methodology and station network;

3) Coda can last for many minutes for large local and regional events, thus allowing the analysis of seismograms with clipped or non-linear main arrivals.

To obtain $M_w(Coda)$ estimates with such methods one does need to first calibrate each station used, which is done by making such measurements on moderate to large ($4 < M_w < 7$) "master events", for which long-period moment-tensor measurements are available. The method used to determine coda magnitude and a review of related coda-magnitude studies will be presented in the next section.

The third and last step, for events without available records to measure coda or other waveform information, is to determine new scaling relations between M_w and the various magnitude scales used as input into the NSHM catalogs, and apply them to the original raw (unconverted) magnitude values used to generate said catalogs in order to provide better moment-magnitude estimates extrapolated from other magnitude measurements. These scaling relations can be determined using both the revised moment magnitudes provided in this study as well as those for events outside of the NSHM catalogs obtained from other source studies; linear regression can then be performed between these values any other particular magnitude scale, using magnitude estimates of said type obtained from various pertinent seismological bulletins. Further, one may apply these robust empirical magnitude scaling relationships to the pre-instrumental earthquakes in the historical catalogs as well, thereby refining the catalog more comprehensively still.

In the following section the development of coda magnitude methods is reviewed, and the rationale for the methods examined in this study are given.

MEASURING CODA MAGNITUDES

Provided here is an overview of the development of coda-based magnitudes, which in turn was basis for the coda magnitude methods examined in this study, the details of which are in the METHODOLOGY and RESULTS section.

Measurements of coda duration, τ , for the purpose of magnitude estimation has a long of history of

use, and has been shown to give reliable results. Herraiz and Espinosa (1987) give a general review of coda waves; Herrmann (1975) provides an overview of coda magnitude studies previous to his on the subject. The most contemporaneous of these studies is Real and Teng's (1973) which related M_L and short-period coda duration for southern California earthquakes, which they found to be:

$$M_\tau = C_0 + C_1 \cdot (\log \tau)^n + C_2 \cdot \Delta \quad (1)$$

where $n = 1$ for $M_\tau \leq 3.8$, and $n = 2$ for $M_\tau > 3.8$ events satisfied their data (note: all references to log terms herein are with respect to log base-ten). They noted that Lee *et al.* (1972), in a study of central Californian earthquakes, found a similar departure from a linear to a quadratic $\log(\tau)$ term in order to fit the duration data of larger magnitude events. Real and Teng speculated that this quadratic term for larger events is attributable to the fact that the M_L scale itself deviates non-linearly from either m_b or M_s for larger magnitude events. A number of other studies examining the relation between coda duration and seismic moment and local magnitude (Bakun and Lindh, 1977; Suteau and Whitcomb, 1979; Bakun, 1984a; and Bakun, 1984b) also found an empirical dependence of seismic moment on a quadratic $\log(\tau)$ term for events with $M > 4$.

Herrmann extended this application of coda-duration magnitude by relating it directly to seismic moment, M_0 , using short-period ($f = 1$ Hz) observations of central and eastern U. S. events. He also found an upturn in the slope of the linear $\log M_0 - \log(\tau)$ relation at $M_w = 3.94$ -- approximately the same magnitude at which the empirical $M_L - \log(\tau)$ relationship found by Real and Teng (1972) requires a quadratic term. This change in the slope of the $M_w - M_C$ relationship was attributed to the convolved effect of source-spectrum corner frequency and instrument bandwidth -- that is, short-period measurements of coda underestimate the source spectrum of larger events with corner frequencies below the peak passband of the recording instrument. In regressing directly versus $\log(M_0)$, however, Herrmann found that a linear $\log(\tau)$ term sufficed to model his observations.

The coda-duration/magnitude relations described above all are empirically based, taking the general form of conventional magnitude equations, with the modification that a $\log(\tau)$ term replaces the usual log amplitude ($\log(A)$) one. Duration has been defined in several ways, but the most appropriate is the coda time minus the origin time ($t_c - t_0$), with t_c defined as the point at which the signal reaches some minimal amplitude, sometimes defined as the pre-transient signal-onset noise level, and sometimes

defined as some slightly higher amplitude, usually the point at which the coda amplitude is some fraction of the peak S-wave amplitude, or at some multiple of the S-wave travel time, *e. g.* twice the S-wave travel time. Aki and Biswas (1984) modified this duration measuring convention by measuring both the coda amplitude and its duration at any point in the later-arriving wave train, and related these combined measurements to seismic moment; for their range of moments, however the log duration term remained linear.

Aside from the method of Aki and Biswas (1984), all the aforementioned studies included a distance term, although the distance dependence was found to be weak. Aki and Chouet (1975) developed a description for coda waves in terms of scattering theory, based on the observations of Aki (1969) that local coda wave amplitude, in the 1-24 Hz passband, was primarily a function of coda duration, and was found in these previous studies to be only weakly dependent on distance from the source. These coda waves are explained in terms of back-scattered waves -- primarily shear -- caused by heterogeneities distributed more or less uniformly in the lithosphere. Rautian and Khalturin (1978) provided additional evidence supporting this interpretation of coda waves in an independent study. This theory implies that coda amplitude decay is a function of lapse time (time after origin) and that this curve is similarly shaped, *i. e.* parallel, for all events within a region, irrespective of the location of the source and the receiver; there is, however, a multiplicative offset factor related to the difference in source excitation and a receiver site correction. The validity of this characteristic of coda-wave amplitude decay has been demonstrated from observations from a variety of regions of the earth by the above authors. Further, Aki (1980) showed that the attenuation (Q^{-1}) of *S* waves has similar frequency dependence to that of coda waves; synthesizing these results Aki (1981) concluded that coda waves are S-to-S back-scattered waves.

By this theory coda amplitude is represented by

$$A(\omega | \tau) = c \tau^{-a} e^{-\omega\tau^2/Q} \quad (2)$$

where the τ^{-a} term represents the effect of geometric spreading, whereas the second, exponential term represents attenuation, which can be simplified with the substitution $b = \log_{10}(e) \cdot \pi f / Q$. At lapse times sufficiently greater than the *S* arrival, and correcting for local geology site effects site effects, coda wave energy is observed to be homogeneously distributed in the crust (Aki, 1969; Aki and

Chouet, 1975; and Mayeda *et al.*, 1992).

Mayeda (1993) applied this theory to NTS explosions recorded by the Lawrence Livermore National Laboratory Seismic Network, and established the following $m_b(Lg\ Coda)$ relationship to coda amplitude and duration:

$$m_b(LgCoda) = \text{Log}_{10}[A_C(\tau)] + \gamma \cdot \log_{10}(\tau) + b \cdot \tau \cdot \log_{10}(e) + C \quad (3)$$

where the γ term represents geometric spreading, and the b term attenuation; $A_C(t)$ is the amplitude of the enveloped coda signal, and C is a constant term. He found these magnitude estimates to be very robust and stable, having 75% to 80% variance reduction in single-station measurements over either $m_b(P_n)$ or $m_b(Lg)$ estimates. This formulation, used for this case in which source-receiver geometry did not deviate significantly between events recorded at any one station, worked well without incorporating a distance correction term, but the author acknowledges that for more general use distance needs to be accounted for, and that certain scattering models are capable of this.

Mayeda and Walter (1996), to this end, refined this method by measuring the coda envelope amplitude in different 20 consecutive bandwidths, between 0.05 and 10 Hz, and employing a 2-D scattering model (Shang and Gao, 1988) which determines the energy density $E(r,t)$, thus implicitly accounting for distance; in addition to which empirical Green's function corrections are made for each passband. This method proved very effective at estimating seismic moments; however, it requires digital data.

Given that the current study entails analysis of analog as well as digital data, this latter method cannot be employed, as we desire one method to apply uniformly to digital and analog waveforms. Therefore in this study we examine the applicability of both the Herrmann (1975) and Mayeda (1993) approaches of estimating seismic moment magnitude (M_w) from time-domain measurements for earthquakes in the western U.S. The former method is more empirical in nature and assumes a distance dependence of coda, whereas the latter relies on the Aki and Chouet (1975) scattering theory which assumes a negligible distance dependence effect, but includes a small linear duration term as well as the $\log(\tau)$ term.

The epicentral distances involved in this study exceed the range to which this scattering theory has

been applied successfully; further, the epicentral distances range widely, some as short as 100 km and others greater than 1000 km. Thus we are examining the possible extension of this latter method which assumes a negligible distance effect; whereas the empirical method, *i. e.* Herrmann (1975) and others, which does include a distance term, is expected to yield accurate magnitude estimates. As will be shown in the METHODOLOGY and RESULTS section, in the final analysis it was found that a hybrid empirical method which incorporates the terms from both these methods, *i.e.* includes both a linear duration and distance term in the magnitude expression, provides the best-fitting model.

DATA

Digital broadband waveform data were collected for earthquakes from the WUS catalog ($M \geq 4$) for the period 1988-1995; these were obtained from IRIS and consist of broad-band, 20 samples/sec recordings. Figure 3 is a map of the western U. S., including the eight seismic stations used and the 224 events analyzed. For the time period examined the WUS catalog contains 260 events; however a large proportion of these additional 36 events had no available record from the network used, *i. e.* they were below the noise level. Of these 36 earthquakes from the WUS catalog, however, 4 were found to be significantly lower in magnitude -- by as much as a full magnitude unit -- and in two cases the events appear non-existent according to the appropriate regional catalogs (see the DISCUSSION section for the details of these particular events).

We constrained the study to the more recent portion of the WUS events as a larger proportion of them have independent moment estimates to be used as GT information for calibration purposes. With this data set we intend to determine which coda magnitude calculation method works the best, and then use these data to calibrate the stations used. These stations are ones that both are currently recording digitally and which were once analog-recording WWSN sites as well.

The seismograms were de-trended, had instrumental effects removed and were then convolved with a WWSP instrument. Their envelopes were then computed, smoothed over a 10-sec window and decimated to 1 sample/sec, producing, in most cases, smooth and well-defined coda curves. The coda envelope curves were averaged over the three components (NS, EW and Vertical) when all were available; otherwise fewer components were accordingly used and normalized accordingly. Coda

amplitudes (cm) and their associated duration times (sec) were then measured and picked by visual inspection. A measurement would be picked from the envelope curves past any incoming phases, where the slope of the coda curve (in log amplitude) is stable, corresponding to the group velocity window of 0.5 to 3.0 km/s, depending on distance. The signal processing and measurements were done using SAC (Lawrence Livermore National Laboratory).

Figure 4a provides an example waveform, its envelope, and the portion of the seismogram over which coda amplitude is measured. Figure 4b compares the envelope to the absolute value of the time series; the peak amplitude measurement of the time series is essentially equivalent to that of the envelope value as is expected. Thus for the purposes here, these two type of measurements -- either digital smoothed envelopes or direct time-domain amplitude measurements -- can be used interchangeably; consequently this method can be applied to analog WWSP data

METHODOLOGY and RESULTS

The first step was to obtain actual moment magnitudes for a sub-population of WUS events to be used as "master events" for calibrating the coda/moment-magnitude equations. Seismic moments were taken from a variety of source studies (Thatcher and Hanks, 1973; Patton and Zandt, 1991; Zhao and Helmberger, 1994; Thio and Kanamori, 1995; and Zhu and Helmberger, 1996), the ISC and BSN seismic bulletins (Pasayanos *et al.*, 1996) and a previous moment compilation by Woods *et al.* (1995), yielding 85 1988+ events with digital recordings as well as another 48 pre-1988 analog-recorded events; multiple moment estimates for a single were averaged. These then are the most reliable formal moment estimates for these earthquakes; moment magnitudes for these events are referred to as "ground-truth" (GT) in the text and figures.

We investigated the behavior of the coda duration and amplitude with respect to both coda-magnitude relations described previously, *i. e.* equations (1) and (3), as we are trying to ascertain the best general method for obtaining coda-based seismic moment. The difference between these two coda magnitude relations is that one has a linear duration term and the other a linear distance term; they are referred to as the DUR and DIST models respectively. We further decided try a hybrid 4-variable variation on the methods which has linear terms in both duration and distance; this is an extension of

current coda magnitude measures. Thus the most general form of the equation relating $\log(M_0)$ to coda amplitude and duration is:

$$\log_{10}(M_0) = a_0 + a_1 \cdot \log_{10}(\tau) + a_2 \cdot \tau + a_3 \cdot \Delta. \quad (4)$$

This is for the 4-variable case; for the DUR case $a_2 \neq 0$ and $a_3 = 0$, whereas for the DIST case $a_2 = 0$ and $a_3 \neq 0$. The expression for the DIST case reduces to equation (1) when the exponent of the $\log(\tau)$ term in the latter expression, n , equals 1; and hence the DIST case is equivalent to Herrmann's (1975) formulation for coda magnitude. The DUR case is essentially the same as equation (3) with $a_2 = b \cdot \log_{10}(e)$, the difference being that equation (3) relates these coda terms to a magnitude scale whereas we are relating them directly to seismic moment.

We chose to directly analyze the empirical relationship between these coda measurements and $\log(M_0)$, rather than M_w , and then converted these moments to M_w using the relationship:

$$M_w = \left(\frac{\log M_0}{1.5} \right) - 10.73, \quad (5)$$

(Kanamori, 1977). As in the coda scattering theory discussed above, the coda duration is directly proportional to seismic moment; thus the relationship we employ has some physical basis, and is not just a purely empirical magnitude relationship.

We employed a combination of methods to determine the coefficients for the magnitude relationships. For the DIST case direct linear 3-variable regression and formal error estimation (Guttman *et al.*, 1965) were performed. Both the DUR and the hybrid 4-variable cases have terms in $\log(\tau)$ and τ , which are not distinctly linearly independent variables; hence we applied a parameter-space, grid-search error minimization (EM) technique to determine the parameters in these cases. However, we did also apply linear regression to the DUR case as a check against the error minimization results; both methods yielded comparable values. The linear regression has the advantage of being less susceptible to the effects of spurious data than the grid-search error minimization method, thus yielding more robust results; one or more extreme spurious data points would cause the grid-search error-minimization to not converge, whereas the least-squares method, even in such cases, yield results similar to those expected without the spurious data. Hence the linear regression for the DUR

case, if not mathematically robust because two of the variables aren't fully linearly independent, does help to identify bad observations, as well as providing an estimate of the bounds on the coefficients. Also as a check of the stability of the error minimization method, we compared the two types of results for the linear DIST case; these values were similar for all stations, suggesting that the multi-variable error minimization method used furnishes stable and reliable results when spurious data are removed.

We examined the behavior of these coda-magnitude relationships for each of the eight stations' data sets, *i. e.* for CMB, PAS, PFO, ALQ (ANMO), COR, GSC, ISC, and TUC. Table 1 provides the results of these analyses. Each set of four entries is for one station, the name of which and the number of observations for being given in column 2; the next four columns give the determined values of the coefficients in equation (4); the last column has the standard error of the estimate for the error-minimization cases. The top entry row is, in each station's case, for the regression results using the the 3-variable DIST model, right below which in the same row, is the estimated error. The next row entry gives the error minimization results for the same case; note the similarity between these two sets of results, thereby confirming the reliability and stability of the error minimization technique. The next row gives the 3-variable DUR coefficient values, and the last gives the 4-variable hybrid method values. The estimated errors in the linear regression case vary between 5 and 20 percent for a_0 and a_1 , but range from 15 to 75% for a_3 , the linear distance term. We did not provide the results of the quasi-linear 3-variable DUR case, as they are not mathematically robust, *i. e.* distinctly linearly independent; however the estimated errors were all approximately twice as large as for this case, often being larger than the linear duration coefficient itself.

The range of variation in coefficient values between stations for each case is fairly small for the terms a_0 and a_1 , being less than 25 percent. This variation is smallest for the 3-variable DIST case, with a_1 varying closely about 5.0, suggesting that this relationship is robust and more consistently models the observations compared to the 3-variable DUR case for which the variation is between 3.53 and 5.15. The variation is larger for the linear duration and distance coefficients terms, a_2 and a_3 respectively. The linear regression DIST results for a_3 suggest relatively large error, so this is not a surprising feature; that this term is negative, however, is somewhat so and will be discussed further.

Comparing these coefficient results to their corresponding representative values in other studies, we

find that the $\log(\tau)$ coefficients, when converted from $\log(M_0)$ to M_w , are not too different from the average value of 2.5 Mayeda (1993) obtained for NTS explosions, being 3.33 on average; however values for the a_2 coefficient, corresponding to his b term (see equations (1) and (2)), are somewhat smaller, being on the order of 50 to 75 percent of the values he obtained for the LANL stations. He however was using virtually constant-length paths for his observations of NTS events, and given that he included no distance term, any effect of this would be taken up by the linear duration coefficient.

For the DIST case, the $\log(\tau)$ coefficients are comparable to those found by Herrmann (1974) for $M_w \geq 3.94$ events, *i. e.* approximately equal to 5. In his study, which involved events as small as $m_b = 2.5$, a break in the slope of the $\log\tau$ - $\log M_0$ curve was observed at $\log(M_0) = 22$ (dyne-cm), ($M_w = 3.94$). Most of the events examined in this study are above this magnitude threshold, and so it was not possible to ascertain whether or not this feature is observed in WUS earthquakes. Values of the distance coefficient term, a_3 are also comparable to that found by Herrmann, which he also found could be negative.

Given the general compatibility of results here with those of these two studies, we conclude that our results are robust and stable.

For the 4-variable case, the $\log(\tau)$ coefficient (a_1) is generally intermediate in value compared to the 3-variable DIST and DUR cases, whereas the a_2 and a_3 terms are comparable to their respective 3-variable-case values. The standard errors of estimate for the 4-variable case are the smallest on average, with the 3-variable DIST case having intermediate values compared to the 3-variable DUR values which are as much as 22 percent larger than the next worse case. These results suggest that the 4-variable $\log M_0$ -coda relation provides the best model of the three methods, with the 3-variable DIST case being second best. However, to ascertain which method provides the best coda-magnitude relation, we performed linear regression analysis on their single-station M_w estimates for each event vs. its respective GT M_w from the master-event list described earlier; this was done for each of the three cases examined.

Figure 5 gives these comparative regression results for the stations PAS and ISA. Figure 5a is a regression plot of GT M_w to the WUS catalog (USGS) value; the sharp cut-off in M_w (USGS) values at $M_w = 4$, is due to constraining the analysis to events listed as $M_w \geq 4$ in this catalog. Figure 5b is the

regression plot for the 3-variable DUR case; the variance is slightly larger than for the case of the USGS M_w 's, with a standard error of estimate of 0.23 versus the former's value of 0.21. Results for the 3-variable DIST case are given in Figure 5c; the standard error in this case is 0.16 magnitude units. For the 4-variable case, Figure 5d, the resulting correlation is drastically improved over the other cases, with a standard error (s. e.) of 0.04 units, a 75 percent reduction in error over the next best results.

Figures 5e-h give analogous plots for the station ISA. In this case the 4-variable and 3-variable DIST results have comparably smaller s. e.'s than the M_w (USGS) catalog values or the 3-variable DUR results; however the larger magnitude ($M_w > 6$) events, albeit a small number of them, show less deviation from the best-fitting curve for the 4-variable case than for the 3-variable DIST case. Further, the scaling relationship slope is closer to unity for the 4-variable case than for the 3-variable DIST one; thus even for this station the 4-variable model provides the best estimates of GT M_w of the three coda-magnitude methods examined. Of the other six stations, only GSC gave the same dramatic variance reduction of PAS for the 4-variable model; however, this model also did still provide an improved estimate of M_w for the reasons cited for the station ISA. Consequently the 4-variable model was chosen to obtain $\log(M_0)$ measurements which were then in turn converted to M_w .

The final 4-variable regression results, in plotted form, are provided in Figure 6a-h. Not all the scaling relationships are as close to unity as in the cases of PAS and GSC, however the estimates of standard error in all cases are significantly reduced -- by at least 25% if not considerably more -- relative to the WUS catalog values; further, the scaling relationship slopes are closer to unity for the magnitude values than the WUS values. Hence the coda-based M_w 's are considered to be an improvement over the current WUS values -- if not also superior moment-magnitude estimates in general.

It should be kept in mind that these regression results for the coda magnitudes are single-station estimates; network-averaged values should provide superior correlation with their GT counterparts. Such results will be shown and discussed later (see Figure 8), but first the inter-station coda M_w relations for these 8 stations are examined; interstation correlations are one measure of how robust these coda-magnitude measurements are.

Inter-station results between PAS and the other 7 analyzed stations are shown in Figures 7a-g. This

comparison to PAS is made since it has been running the longest -- at least with respect to digital broad-band recording -- and thus has the most comprehensive number of such moment estimates. For some of these regression plots there are events distinctly in the $M_w < 3.5$ ranges; these are for events which in fact had considerably smaller magnitudes than their WUS catalog entries. These events and other small or "phantom" events in the WUS catalog will be described in the DISCUSSION section.

Figure 7h provides the inter-station correlation of ALQ (ANMO) and COR, the two most geographically separated stations (see Figure 3). Not surprisingly, this last comparison yields the largest standard error and the scaling relationship which deviates most from unity, but still the result is better than the GT-WUS comparison. The correlations between PAS and the other stations are all considerably better than the GT-WUS correlation; this is particularly true for the case of GSC, with a correlation coefficient of 0.99; however the other correlations are all quite high, being in the 98th percentile or higher. The estimated standard errors are all smaller than that for the relationship between the current WUS catalog and GT M_w 's; therefore we treated the moment estimates from each station equally, and went on to average them over this working network of eight stations for the final M_w catalog results.

Finally, the network-averaged M_w 's are compared to the other M_w estimates. Figure 8a is a plot of $M_w(GT)$ vs. $M_w(coda)$. The correlation is high, in the 99th percentile; and the estimated standard error is 0.11 magnitude units. The slope, however, is slightly less than unity. Applying a fixed slope of unity to the regression (Figure 8b) of the same data suggests that it is the larger magnitudes events ($M_w > 6.5$), which have slightly decreased magnitude with respect to their $M_w(GT)$, which depress the free-slope regression result. In both cases the standard error is relatively small, approximately half that for the $M_w(USGS)-M_w(GT)$ (Figure 8d). For the sake of comprehensiveness, the network-averaged M_w 's were also regressed vs. $M_w(USGS)$ for the master-event population. Not surprisingly the variance in this regression result is fairly large, no better than that between $M_w(USGS)$ and $M_w(GT)$.

The final network-averaged coda-based moments for 224 western U. S. earthquakes and their statistics are provided in terms of moment magnitude in Table 2. For the sake of consistency it was decided to use only the coda-measured M_w 's rather than incorporating the GT moments themselves. The GT M_w 's for the 80 master events are given as well in a separate column Table 2.

DISCUSSION

The results described above suggest that coda duration/amplitude measurements provide good estimates of seismic moment -- significantly better than just converting other magnitudes to one universal one, *e. g.* M_w . Further, the individual station magnitude estimates are quite stable and robust; therefore this method can be successfully applied to events with few or even single observations.

One result of the study, however, requires further discussion; that is the negative distance-term coefficient for most all of the stations. On the face of it, this seems counterintuitive as attenuation and geometric spreading effects should cause amplitude to decrease with distance. However, in the single-scatter theory of Aki and Chouet (1975), which corresponds to the DUR-case coda magnitude relation, the $\log(\tau)$ and τ term represent geometrical spreading and frequency-dependent attenuation, respectively. Thus these terms account for the usual distance effect of most magnitude relations.

The physical feature being measured, coda wave amplitude, is understood to be coupled to scattering processes. The number of significant scatterers a wave field encounters will increase with the distance it propagates. For the single-scatter model, the loci of scattering points with coincident arrivals are given by an ellipse, the foci of which are the source and receiver; as the distance between them increases, the circumference of the ellipse does as well, generating more scatterers. It could be that such off-azimuth scatterers can increase the coda amplitude with distance propagated but that this effect is small, *i. e.* overwhelmed, by geometric spreading and anelastic attenuation, and thus not readily observable; none the less, the distance effect by itself may increase scatter-based coda amplitude in high-scattering regimes.

Generally, of course, distance terms for magnitude scale, are meant to model the propagation character of a distinct phase or wavetrain which attenuates with distance, due to intrinsic Q , or anelastic attenuation, as well as to scatter Q . For scattered coda waves, however, we are modeling a phase or wavetrain which is generated from scattered waves. In a region in which a large proportion of effective Q is due to scattering, it may be that up to some range that the scattered energy builds up with distance, with the scattering effect outweighing the anelastic attenuation upon these scattered waves. Such may be the case for the western U. S., known for the heterogeneity of its upper crust.

The empirical evidence found in this study supports this thesis. Keep in mind that this distance term has the smallest coefficient in the magnitude relations obtained, being on the order of -5×10^{-4} . Further analysis of larger data sets, preferably with certain source-receiver geometries, as well as studies in regions where scattering Q is believed to be lower, *e. g.* the eastern U. S., could shed more light on this phenomenon. That the one station with a positive distance-term coefficient is ALQ/ANMO, on the Colorado Plateau, a more homogeneous crustal region with less apparent scattering Q (Mayeda and Walter, 1996), suggests this is the case.

One striking result is the correlations with the GT M_w 's for the PAS and GSC coda M_w 's relative to the other stations. It is not surprising that data from geographically disparate stations from those in Southern California, *i. e.* CMB, TUC, ALQ and COR, would perhaps be harder to fit with this the same coda-magnitude model, that the other southern Californian stations ISA and PFO yield no better fitting results is. There are two primary explanations. The first is that there may be pronounced azimuthal station effects (corrections), due to crustal waveguide about the stations which exhibit larger variation in M_w . That this effect would be minimal at two stations and then significantly larger -- and all comparable in size -- for the other six stations makes this seem unlikely; one would expect more variation in the variance between stations.

The second and more likely reason is that there was some difference in the measuring of the coda amplitude and duration between PAS and GSC, and the other six stations. All data was processed in the same fashion; however there was a quality-checking step in which spurious data were re-examined and either culled or remeasured while checking for misidentified events. This was done, in part, by examining inter-station plots of M_w , and looking for outliers. PAS was used, when possible, as one station of the pair in this procedure as it was one of the first running broadband digital stations, and hence recorded the greatest number of events being examined. Consequently, any spurious PAS data were more likely to be found and dealt with appropriately. Similarly GSC, the second-longest running station, was used as a back up for cases in which PAS had not recorded the event, and so the GSC data were also better checked. Thus this effect may be do to picking judgement.

To achieve this level of accuracy in estimating M_w for all stations could likely be achieved by introducing a correction for the background noise level of the seismogram. In some cases the ambient

signal is half the amplitude of the coda signal -- a 0.3 difference in log amplitude and log moment or 0.2 M_2 units. This would improve the magnitude estimates of both smaller events as well as more distant observations of moderate-sized earthquakes.

This study made use of more distant ($R > 600\text{km}$) regional seismograms than past coda-magnitude studies; this entailed extending duration measurements as well to times as great as 600 to 900 secs. The window chosen, as late in the coda as possible given noise-level considerations, corresponded to group velocities that, on average, grew with epicentral distance. For distances less than 300 km, the range was approximately between 0.5 and 1.0 km/s. Duration measurements of less than 100 sec. underestimated the magnitude; consequently none were not used, but rather measurements were made later in the coda. Group velocities for the coda in the intermediate distance range ($300\text{ km} < R < 600\text{ km}$) vary between 1.0 and 2.0 km/s. These two types of observations are in agreement with those of Meyada (1993). Additionally, coda wave-train group velocities for the more distant ($R > 600\text{ km}$) events range between 2.0 and 3.0 km/s. Magnitude estimates made from these more distant observations are consistent with nearer ones.

The limit on these more distant measurements is determined by the decay of the short-period S wave. In the western U. S., a region known for high S-wave attenuation, this phase's wave train generally drops below the noise level past 1100-1400 km for even moderate-sized ($M_w < 5$) earthquakes, which then is the approximate measuring threshold limit for this magnitude. For the eastern U. S., where S-wave attenuation is less, this threshold may be extended somewhat; that and smaller events will be observable at a greater distance than comparable-magnitude western U. S. earthquakes.

One other topic that needs to be addressed is the apparent inaccuracies in the WUS catalog; this was found to be the case for 6 events. Four of the events were, in fact, of considerably lower magnitude than their WUS value; in two cases the events were found in neither of three appropriate local or regional catalogs, *i. e.* that of the University of Nevada, RENO (UNR); the Southern California Seismic Network (SCSN); and University California, Berkeley (UCB), bulletin; nor in the ISC or PDE bulletins. Table 3 provides the WUS entry as well as those from these networks' bulletins when available. The problematic events all had been reported by the CDMG; however other CDNG-reported

magnitudes in the WUS catalog were correct.

CONCLUSION

We have developed a method for estimating moment magnitude, M_w , from measurements of coda duration and amplitude, using regional short-period seismograms. This method is a hybrid of other coda magnitude measurements, which provides improved estimates of M_w or $\log(M_0)$. As this method uses time-domain measurements from a short-period seismogram, it is quite useful for obtaining moment estimates of smaller earthquakes, for which it is not possible to obtain longer-period (3-30 sec) moment-tensor-based estimates of M_w . It appears that larger events ($M_w > 6.5$) may have their magnitude slightly underestimated, but the level of "saturation" in the coda-magnitude measurement is much less than for the case of m_b or M_L ; hence it is an attractive alternative measure to quantify earthquakes than these latter two magnitude types.

The M_w estimates correlate well with master-event M_w 's, even for single-station estimates, better than the current WUS catalog values do, although this new coda magnitude is still not as comprehensive due to data availability and station coverage. However, by comparing our available M_w estimates with those from the current WUS catalog, inferences can be made to correct the values in this latter catalog for other non-instrumentally recorded events. Although measurements were confined to digital seismograms for this report, we showed that the method is equally applicable to analog records such as those from WWSP stations.

We have compiled our network-averaged M_w values into one catalog, available electronically, for interested parties to update the NSHM WUS catalog, as well as for general use of the seismological community.

Because of the stable and robust single-station estimates of moment magnitude this method provides, it could have considerable application to the field of seismic monitoring as $m_b:M_w$ is one of the more dependable seismic discriminants (Patton and Walter, 1993; and Woods *et al.*, 1993), and coda M_w would be a good measurement to apply in this discriminant to small and/or distant events.

REFERENCES

- Aki, K., 1969. Analysis of the seismic coda of local earthquakes as scattered waves, *J. Geophys. Res.* **74**, 615-631, 1969.
- Aki, K. and B. Chouet, 1975. Origin of coda waves: source, attenuation, and scattering effects, *J. Geophys. Res.* **80**, 3322-3342.
- Aki, K., 1980. Attenuation of shear waves in the lithosphere for frequencies from 0.05 to 25 Hz, *Phys. Earth Planet. Interiors* **21**, 50-60.
- Aki, K., 1981. Attenuation and scattering of short-period seismic waves in the lithosphere, in *Identification of Seismic Sources -- Earthquakes or Underground Explosion*, E. S. Husebye and S. Mykkeltveit, Editors, D. Reidel Publishing Co., Dordrecht, The Netherlands.
- Bakun, W. H. and A. G. Lindh, 1977. Local magnitudes, seismic moments, and coda durations for earthquakes near Oroville, California, *Bull. Seism. Soc. Am.* **67**, 615-629.
- Bakun, William H., 1984a. Seismic moments, local magnitude and coda-duration magnitudes for earthquakes in central California, *Bull. Seism. Soc. Am.* **74**, 439-458.
- Bakun, William H., 1984b. Magnitudes and moments of duration, *Bull. Seism. Soc. Am.* **74**, 2335-2356.
- Biswas, N. N. and K. Aki, 1984. Characteristics of coda waves: central and south-central Alaska, *Bull. Seism. Soc. Am.* **74**, 493-507.
- Bolt, B. A. and M. Herraiz, 1983. Simplified estimation of seismic moment from seismograms, *Bull. Seism. Soc. Am.* **73**, 735-748.
- Frankel, A., 1995. Mapping seismic hazard in central and eastern United States, *Seism. Res. Letts.* **66**, pp. 8-21.
- Frankel, A., C. Mueller, T. Barnhard, D. Perkins, E. V. Leyendecker, N. Dickman, S. Hanson, and M. Hopper, 1996. Interim National Seismic Hazard Maps: Documentation, U.S. Geological Survey, Open-File Report 96-S32 (<http://gldage.cr.usgs.gov/eq/hazmapsdoc/>), 100p.
- Guttman, I., S. S. Wilks, and J. S. Hunter, 1965. Introductory Engineering Statistics, *John Wiley & Sons*, pp. 369-373.
- Herraiz, M. and A. F. Espinosa, 1987. Coda waves: a review, *Pure and Applied Geophys.*, **125**, 499-577.
- Herrmann, R. B. 1975. The Use of duration as a measure of seismic moment and magnitude, *Bull. Seism. Soc. Am.* **65**, 899-913.
- Kanamori, H., 1977. The energy release in great earthquakes. *J. Geophys. Res.*, **82**, 2981-2987.
- Kanamori, H., J. Mori, E. Hauksson, T. H. Heaton, L. K. Hutton, and L. M. Jones, 1993. Determination of earthquake energy release and M_L using TERRASCOPE, *Bull. Seism. Soc. Am.* **83**, 330-346.
- Mayeda, K., S. Koyanagi, Hoshiba, K. Aki and Y. Zeng, 1992. A comparative study of scattering, intrinsic, and coda Q^{-1} for Hawaii, Long Valley and central California between 1.5 and 15.0 Hz, *J. Geophys. Res.* **97**, 6643-6659.
- Mayeda, K., 1993. mb(LgCoda); A stable single station estimator of magnitude, *Bull. Seism. Soc. Am.* **83**, 851-861.

- Mayeda, K. and W. Walter, 1996. Moment, energy, stress drop, and source spectra of western United States earthquakes from regional coda envelopes, *J. Geophys. Res.* **101**, 11,195-11,208.
- Mueller, C., H. Hopper and A. Frankel, 1997. Preparation of earthquake catalogs for the National Seismic Hazard Maps: Contiguous 48 States. U.S. Geological Survey Open-File Report 97-464 (<http://geohazards.cr.usgs.gov/eq/Mf97-464>).
- Pasayanos, M. D., Dreger and B. Romanowicz, 1996. Toward Real-Time Estimation of Regional Moment Tensors, *Bull. Seism. Soc. Am.*, **86**, 1255-1269.
- Patton, H. J. and G. Zandt, 1991. Seismic moment tensors of western U. S. earthquakes and implications for tectonic stress field, *J. Geophys. Res.* **FR**, **96**, 18,245-18,259.
- Patton, H. J. and W. R. Walter, 1993. Regional moment:magnitude relations for earthquakes and explosions, *Geophys. Res. Letts.*, **20**, 277-280.
- Rautian, T. G. and V. I. Khalturin, 1978. The use of the coda for determination of the earthquake source spectrum, *Bull. Seism. Soc. Am.* **68**, 923-948.
- Shang, T. and L. S. Gao, 1988. Transportation theory of multiple scattering and its application to seismic coda waves, *Sci. Sinica (Series B)*, **31**, 1503-1514, 1988.
- Singh, S. and R. B. Herrmann, 1983. Regionalization of crustal coda Q in the continental United States, *J. Geophys. Res.* **88**, 527-538.
- Suteau, A. M. and J. H. Whitcomb, 1979. A local earthquake coda magnitude and its relation to duration, moment M_0 and local Richter magnitude M_L , *Bull. Seism. Soc. Am.* **69**, 353-368.
- Thatcher, W. and T. C. Hanks, 1973. Source parameters of Southern California earthquakes, *J. Geophys. Res.* **78**, 8547-8576.
- Thio, H. K. and H. Kanamori, 1995. Moment-tensor inversions for local earthquakes using surface waves recorded at TERRASCOPE, *Bull. Seism. Soc. Am.*, **85**, 1021-1038.
- Woods, B. B., S. Kedar and D.V. Helmberger, 1993. $M_L:M_0$ as a regional seismic discriminant, *Bull. Seism. Soc. Am.*, **83**, 1167-1183.
- Zhao, L. S. and D. V. Helmberger, 1994. Source estimation from broadband regional seismograms, *Bull. Seism. Soc. Am.*, **84**, 91-104.
- Zhu, L. and D. V. Helmberger, 1996. Advancement in source estimation techniques using broadband regional seismograms, *Bull. Seism. Soc. Am.*, **86**, 1634-1641.

Table 1: Coda Magnitude Calibrations for western US Stations					
Model	Station	a_0	a_1 : $\log(\tau)$	a_2 : τ	a_3 : Δ
3-var linear regression	PAS	8.67 ± 0.63	5.56 ± 0.294	–	$-8.92e-4$ $\pm 1.96e-4$
3-var E. M. (Dist.)	no. of	8.70	5.55	–	$-9.10e-4$
3-var E. M. (Dur.)	obs.	11.90	3.95	1.50e-3	–
4-var Error Min.	= 72	10.60	4.60	1.35e-3	$-9.50e-4$
3-var linear regression	GSC	9.07 ± 1.05	5.31 ± 0.488	–	$-7.48e-4$ $\pm 1.30e-4$
3-var E. M. (Dist.)	no. of	9.20	5.25	–	$-7.30e-4$
3-var E. M. (Dur.)	obs.	12.70	3.53	2.50e-3	–
4-var Error Min.	= 48	11.50	4.10	1.79e-3	$-8.50e-4$
3-var linear regression	ISA	10.01 ± 0.927	4.97 ± 0.430	–	$-4.82e-4$ $\pm 3.12e-4$
3-var E. M. (Dist.)	no. of	10.05	4.95	–	$-4.70e-4$
3-var E. M. (Dur.)	obs.	12.15	3.88	2.25e-3	–
4-var Error Min.	= 50	12.40	3.70	2.32e-3	$-6.10e-4$
3-var linear regression	PFO	9.05 ± 0.797	5.43 ± 0.368	–	$-8.51e-4$ $\pm 2.32e-4$
3-var E. M. (Dist.)	no. of	9.0	5.45	–	$-8.50e-4$
3-var E. M. (Dur.)	obs.	12.40	3.73	2.25e-3	–
4-var Error Min.	= 45	10.40	4.75	1.00e-3	$-8.50e-4$
3-var linear regression	CMB	10.29 ± 0.905	4.89 ± 0.427	–	$-5.07e-4$ $\pm 2.87e-4$
3-var E. M. (Dist.)	no. of	10.25	4.90	–	$-5.00e-4$
3-var E. M. (Dur.)	obs.	11.15	4.45	$-5.00e-4$	–
4-var Error Min.	= 67	13.60	3.10	3.95e-3	$-1.07e-3$
3-var linear regression	TUC	9.61 ± 1.18	5.08 ± 0.497	–	$-5.52e-4$ $\pm 2.59e-4$
3-var E. M. (Dist.)	no. of	9.55	5.10	–	$-5.50e-4$
3-var E. M. (Dur.)	obs.	12.65	3.58	2.00e-3	–
4-var Error Min.	= 33	10.10	4.85	2.10e-4	$-5.40e-4$
3-var linear regression	ALQ	8.76 ± 1.13	4.99 ± 0.454	–	$2.66e-4$ $\pm 2.22e-4$
3-var E. M. (Dist.)	no. of	8.75	5.00	–	$2.60e-4$
3-var E. M. (Dur.)	obs.	8.65	5.13	2.50e-4	–
4-var Error Min.	= 55	10.10	4.40	4.70e-4	$2.80e-4$
3-var linear regression	COR	8.70 ± 1.84	5.38 ± 0.742	–	$-5.36e-4$ $\pm 2.68e-4$
3-var E. M. (Dist.)	no. of	8.65	5.40	–	$-5.30e-4$
3-var E. M. (Dur.)	obs.	9.00	5.15	$-7.50e-4$	–
4-var Error Min.	= 27	10.25	4.65	8.80e-4	$-5.40e-4$

Table 1. Station calibration results for the various coda magnitude equations examined. Each set of four entries is for one station; the top set are for the 3-variable linear regression involving $\log_{10}(\tau)$ and Δ , next are the corresponding 3-variable error minimization (E. M.) results, followed by those for the case involving $\log_{10}(\tau)$ and linear τ , and last the full 4-variable error minimization results including both linear τ and Δ .

Table 2: Network-averaged Coda M_w 's and available GT M_w 's							
Date	Hr:Min	Longitude	Latitude	M_w	σ	n	M_w (GT)
88/05/14	00:58	-109.7000	25.5700	4.81	-	1	-
88/05/26	03:56	-117.8318	37.0905	3.79	-	1	-
88/06/10	23:06	-118.7427	34.9430	5.43	0.127	2	-
88/06/11	08:58	-109.3340	30.7740	4.42	-	1	-
88/06/13	01:45	-121.7403	37.3927	4.92	0.028	2	4.97
88/06/18	22:49	-110.9960	26.8560	6.57	0.049	2	6.63
88/06/19	07:26	-112.3790	27.5070	4.31	-	1	-
88/06/21	07:34	-110.9610	26.2980	4.57	-	1	-
88/07/02	00:26	-116.4385	33.4832	4.03	-	1	-
88/07/05	18:18	-118.0255	36.4258	4.36	0.205	2	-
88/07/14	17:31	-114.0830	44.4560	4.84	-	1	4.59
88/07/20	14:05	-109.7310	25.1470	4.10	-	1	-
88/07/29	04:59	-121.9140	46.8540	4.30	-	1	-
88/09/19	02:56	-118.3420	38.4610	4.68	-	1	-
88/09/30	00:30	-121.5893	41.5823	4.47	-	1	4.34
88/11/13	11:53	-110.9740	42.6360	4.09	-	1	-
88/11/19	19:42	-111.4720	41.9960	4.99	0.290	2	-
88/11/20	05:39	-118.0712	33.5073	4.78	-	2	-
88/11/22	07:57	-118.5600	37.4028	4.04	-	1	-
88/12/16	05:53	-116.6813	33.9788	4.79	0.198	2	-
89/01/09	23:01	-120.7015	34.5132	4.37	-	1	-
89/01/15	15:39	-117.7363	32.9475	4.37	-	1	-
89/01/19	06:53	-118.6275	33.9187	5.02	0.134	2	5.01
89/01/22	19:15	-110.3490	26.0830	4.07	-	1	-
89/01/30	04:06	-111.6140	38.8240	5.23	0.134	2	5.22
89/02/14	21:41	-122.2280	48.4290	4.15	-	1	-
89/03/05	00:40	-112.2570	35.9520	4.16	-	1	-
89/03/18	11:20	-113.1920	25.0180	4.44	-	1	-
89/03/29	09:29	-118.9923	34.9140	3.98	-	1	-
89/04/03	17:46	-121.7700	37.4322	4.92	-	1	4.84
89/04/20	12:45	-117.8060	38.4940	4.14	0.007	2	-
89/05/25	07:43	-109.3320	30.8460	4.75	-	1	-
89/06/02	09:55	-121.0000	40.2160	3.93	-	1	-
89/06/04	21:33	-116.8385	34.5967	4.17	-	1	-
89/06/10	18:35	-124.4127	41.5008	4.39	-	1	-
89/06/11	12:00	-124.8950	44.4770	4.35	-	1	-
89/06/18	20:38	-122.7760	47.4100	4.41	-	1	-
89/06/22	01:13	-121.8515	38.0603	4.26	0.014	2	-
89/06/22	21:06	-114.2620	30.3950	5.07	0.092	2	-
89/06/22	21:28	-114.2040	29.7860	5.01	-	1	-
89/07/03	22:44	-112.3730	41.7060	4.70	0.071	2	-
89/07/11	04:13	-118.6285	37.4280	4.52	-	1	4.36
89/09/21	11:48	-120.4673	39.3748	4.16	0.037	3	4.00
89/09/30	09:21	-120.5200	36.4995	4.11	0.078	2	3.93
89/10/18	00:04	-121.8773	37.0397	6.82	0.080	3	6.90

Table 2. Network-averaged Coda M_w 's for the earthquakes examined, along with other event information. The coda- M_w σ 's are given along with the number of observations. For master events, the ground truth (GT) M_w 's are also provided.

Table 2 (continued): Network-averaged Coda M_w 's and available GT M_w 's							
Date	Hr:Min	Longitude	Latitude	M_w	σ	n	M_w (GT)
89/10/22	02:10	-110.3770	26.3040	5.24	0.120	2	5.29
89/11/03	19:09	-119.6443	38.6035	4.30	0.038	4	-
89/11/12	00:14	-114.0150	30.8710	4.89	0.233	2	-
89/11/26	19:00	-110.0760	25.8920	5.68	0.049	2	5.56
89/11/29	06:54	-106.8910	34.4550	4.92	0.212	2	-
89/12/02	23:16	-116.7417	33.6457	4.26	0.247	2	-
89/12/18	06:27	-116.0238	33.7338	4.18	0.240	2	-
89/12/24	08:45	-122.1160	46.6500	4.88	0.170	2	-
89/12/31	05:46	-118.7920	38.7920	3.89	0.108	3	-
90/01/12	09:10	-120.7850	36.4232	4.37	0.049	3	4.38
90/01/13	05:47	-114.4400	30.2220	4.60	0.137	3	-
90/01/15	05:29	-118.0000	38.1085	4.61	0.060	4	-
90/01/16	20:08	-124.3840	40.2438	5.46	0.034	4	5.47
90/01/18	11:45	-123.7613	41.1737	4.94	0.077	4	-
90/01/27	06:28	-113.7300	30.1210	4.22	0.092	2	-
90/02/06	18:14	-121.0000	34.9533	4.07	-	1	-
90/02/28	23:43	-117.6973	34.1437	5.69	0.154	4	5.55
90/04/07	02:39	-121.9790	37.8755	4.82	0.024	4	4.69
90/04/14	05:33	-122.1610	48.8450	4.72	-	1	-
90/05/01	08:41	-117.6338	32.1000	4.28	0.170	2	-
90/06/11	04:52	-111.2600	27.3940	4.56	-	1	-
90/08/05	21:27	-116.4142	33.3248	3.74	0.057	2	-
90/08/31	03:38	-116.0492	33.2472	4.35	0.304	2	-
90/09/06	05:24	-110.5600	27.1970	4.45	0.042	2	-
90/09/24	09:47	-124.1735	40.7318	3.72	-	1	-
90/10/24	06:15	-119.1570	38.0470	5.25	0.040	5	5.28
90/11/08	10:46	-106.8560	34.4490	4.52	0.202	3	4.25
90/11/28	02:48	-116.4570	38.6730	3.83	0.059	3	-
90/12/13	01:01	-117.4945	37.3200	3.07	0.049	2	-
90/12/18	16:56	-118.8458	35.3742	4.03	0.082	5	3.97
91/01/02	23:16	-119.7330	39.2120	4.70	0.046	6	4.81
91/02/04	16:38	-121.5578	36.0308	4.36	0.053	3	4.58
91/02/14	16:37	-113.8580	29.6810	5.50	0.063	6	5.42
91/02/15	04:56	-113.4020	29.3520	4.73	0.155	4	-
91/02/18	12:51	-113.2580	30.9730	5.02	0.203	4	-
91/02/19	23:04	-122.7250	49.6960	4.11	-	1	-
91/02/22	19:58	-118.3947	38.3430	3.65	0.040	5	-
91/03/10	17:46	-121.7538	37.7050	3.89	0.029	5	4.02
91/03/25	15:46	-118.9418	37.6420	3.95	0.066	6	-
91/05/04	18:28	-118.4297	37.5555	3.95	0.027	5	4.04
91/05/23	04:08	-124.9933	40.7543	3.69	0.205	2	-
91/06/14	04:29	-121.5930	40.7883	3.23	-	1	-
91/06/28	14:43	-117.9995	34.2615	5.74	0.063	5	5.54
91/06/29	17:53	-116.5793	34.9085	3.83	0.038	4	3.63
91/07/04	11:20	-113.8570	30.4460	4.66	0.109	3	-

Table 2 (continued). Network-averaged Coda M_w 's for the earthquakes examined, along with other event information. The coda- M_w σ 's are given along with the number of observations. For master events, the ground truth (GT) M_w 's are also provided.

Table 2 (continued): Network-averaged Coda M_w 's and available GT M_w 's							
Date	Hr:Min	Longitude	Latitude	M_w	σ	n	M_w (GT)
91/07/05	17:41	-118.5555	34.4970	4.00	0.154	4	3.72
91/07/13	02:50	-125.6410	42.1820	6.69	0.043	4	6.83
91/07/17	05:12	-111.6600	27.8080	4.62	0.181	3	-
91/07/19	02:41	-115.9682	33.2125	4.08	0.112	3	-
91/08/02	16:58	-112.4090	26.7300	4.31	0.028	2	-
91/08/11	06:09	-118.8408	37.6268	3.78	0.018	5	-
91/08/12	21:11	-118.7435	38.2195	4.45	0.057	5	4.34
91/09/17	21:10	-121.3335	35.8187	4.89	0.040	6	4.86
91/09/21	09:44	-124.6100	40.6938	4.26	0.093	4	4.08
91/10/12	14:39	-116.1637	33.8902	3.97	0.064	2	3.90
91/11/26	13:31	-110.9120	26.6300	4.99	0.072	3	-
91/11/26	16:18	-124.9545	40.4813	n. l.	-	0	3.30
91/11/28	01:08	-118.3170	45.9900	4.43	-	1	-
91/12/04	07:10	-116.8035	33.0697	3.88	0.032	5	3.81
91/12/04	08:17	-117.0223	34.1777	3.88	0.032	5	3.66
91/12/20	10:38	-117.3713	35.5350	3.89	0.064	5	3.86
91/12/26	00:22	-109.6930	25.3070	4.97	0.071	2	-
91/12/28	07:00	-114.1140	44.5600	4.70	0.028	2	-
92/01/12	23:07	-118.0050	35.7538	4.44	0.099	2	-
92/02/15	14:36	-121.6112	37.6767	4.03	0.042	5	3.92
92/02/19	11:19	-117.8893	36.0258	4.10	0.050	6	3.76
92/03/04	19:06	-118.7908	32.9753	4.14	0.063	4	4.08
92/03/09	04:51	-123.3737	40.5732	4.34	0.042	7	-
92/03/14	05:13	-112.3550	35.9600	4.03	0.063	5	-
92/03/16	14:42	-112.0430	40.4650	4.47	0.075	6	-
92/03/21	01:57	-113.2710	47.2910	4.39	-	1	-
92/04/01	11:33	-113.7290	47.8840	4.41	-	1	-
92/04/04	01:30	-111.0780	43.8320	4.20	0.075	4	-
92/04/04	22:29	-125.6860	45.1560	4.35	-	1	-
92/04/06	04:01	-117.1292	39.5868	4.19	0.091	7	-
92/04/14	01:31	-112.4930	28.1200	5.11	0.090	5	-
92/04/25	18:06	-124.2295	40.3327	6.83	0.059	7	7.04
92/05/04	09:14	-113.9780	44.5100	4.75	0.061	6	-
92/05/11	11:20	-119.5573	38.7320	3.65	0.092	2	-
92/05/22	14:09	-115.0190	27.3590	5.31	0.097	5	-
92/05/22	16:02	-115.1220	26.9760	4.41	0.049	5	-
92/05/24	12:22	-116.1740	32.8215	3.86	0.037	4	-
92/05/25	20:40	-110.4930	26.2140	5.43	0.085	4	-
92/06/28	11:57	-116.4367	34.2002	7.16	0.057	6	7.29
92/06/28	12:34	-118.3540	38.3410	4.33	0.144	4	-
92/06/28	13:28	-116.9043	36.5872	4.42	0.041	7	-
92/06/28	17:16	-116.5255	35.7473	3.85	0.057	7	-
92/06/29	01:18	-117.3620	35.1600	4.38	0.071	7	-
92/06/29	03:36	-116.8002	35.3617	3.95	0.064	7	-
92/06/29	10:14	-116.2930	36.7050	5.59	0.031	7	5.65
92/06/30	13:05	-117.6152	35.6810	4.67	0.052	8	4.58

Table 2 (continued). Network-averaged Coda M_w 's for the earthquakes examined, along with other event information. The coda- M_w σ 's are given along with the number of observations. For master events, the ground truth (GT) M_w 's are also provided.

Table 2 (continued): Network-averaged Coda M_w 's and available GT M_w 's							
Date	Hr:Min	Longitude	Latitude	M_w	σ	n	M_w (GT)
92/07/02	13:59	-121.2097	35.6052	4.22	0.063	7	4.21
92/07/04	08:43	-111.7220	26.9400	4.68	0.088	7	-
92/07/05	18:17	-112.2190	35.9820	3.97	0.050	7	-
92/07/11	18:14	-118.0657	35.2100	5.29	0.017	7	5.17
92/07/16	15:38	-122.0000	40.3238	4.08	0.047	4	-
92/07/17	06:00	-117.6887	37.8523	3.16	0.035	2	-
92/07/20	20:09	-119.1120	39.3150	4.44	0.049	7	-
92/07/21	20:58	-115.6260	39.3560	4.00	0.036	7	-
92/07/27	20:40	-115.6278	32.6122	3.80	0.040	7	3.67
92/07/27	22:10	-117.6787	36.0845	3.90	0.062	6	-
92/07/29	22:24	-117.2870	37.1300	3.73	0.046	7	-
92/08/04	13:38	-117.8965	37.5063	3.90	0.067	7	-
92/08/05	22:22	-116.9523	34.9785	4.44	0.051	7	4.38
92/08/30	01:17	-114.1950	30.1440	4.46	0.058	5	-
92/09/02	10:26	-113.4720	37.0900	5.46	0.040	7	5.55
92/09/16	06:14	-119.9110	36.0000	4.44	0.033	5	-
92/09/19	23:04	-122.7935	38.8598	4.69	0.064	4	4.75
92/10/03	07:37	-111.3640	27.5100	5.42	0.048	6	-
92/10/10	17:54	-118.5800	37.9930	3.94	0.025	5	-
92/10/11	00:55	-111.7820	27.2060	4.63	0.089	4	-
92/10/20	05:28	-120.4725	35.9287	4.37	0.054	5	4.52
92/10/23	05:26	-109.8470	26.1800	4.70	0.068	5	-
92/11/04	18:22	-113.3360	41.4700	4.68	0.051	8	-
92/11/08	02:17	-109.9590	25.9040	4.93	0.163	2	-
92/11/10	10:54	-111.4190	43.0900	4.64	0.078	6	-
92/12/02	07:12	-116.3820	30.3660	4.28	0.050	6	-
92/12/25	04:25	-120.8420	39.9550	3.98	0.022	5	3.78
93/01/15	14:17	-116.3430	39.2050	4.36	0.035	8	-
93/01/16	06:29	-121.4628	37.0192	4.89	0.037	8	5.04
93/02/08	00:53	-115.6620	36.7010	3.87	0.065	7	-
93/02/10	21:48	-119.6120	40.4290	4.66	0.027	8	4.60
93/02/11	12:39	-116.9727	35.0262	4.11	0.055	7	-
93/02/18	16:19	-114.8230	44.5140	4.21	0.124	5	-
93/02/24	04:27	-111.9910	28.3550	4.84	0.067	6	-
93/03/05	08:20	-113.1220	28.7100	5.56	0.073	8	5.69
93/03/25	13:34	-122.6070	45.0350	5.63	0.080	8	5.61
93/04/04	05:21	-120.4925	35.9418	4.28	0.009	5	4.47
93/04/05	07:38	-113.8430	28.4820	4.30	0.040	5	-
93/04/29	08:21	-112.1120	35.6110	5.28	0.038	7	5.31
93/05/17	23:20	-117.7948	37.1680	5.84	0.106	7	6.06
93/05/20	20:14	-117.7018	36.0948	4.52	0.028	6	4.66
93/05/28	04:47	-119.1037	35.1493	4.71	0.030	8	4.75
93/06/02	02:08	-109.9890	25.9460	5.17	0.064	8	-
93/07/08	02:25	-114.2590	29.9230	5.08	0.100	6	-
93/08/11	05:48	-118.8822	37.5278	4.31	0.040	8	4.25

Table 2 (continued). Network-averaged Coda M_w 's for the earthquakes examined, along with other event information. The coda- M_w σ 's are given along with the number of observations. For master events, the ground truth (GT) M_w 's are also provided.

Table 2 (continued): Network-averaged Coda M_w 's and available GT M_w 's							
Date	Hr:Min	Longitude	Latitude	M_w	σ	n	M_w (GT)
93/08/11	22:33	-121.6760	37.3123	4.83	0.018	8	4.88
93/09/21	03:36	-122.0000	42.7170	4.85	0.150	7	-
93/09/21	05:45	-122.0000	42.3085	5.93	0.037	8	6.00
93/09/22	07:01	-116.2100	37.2010	4.20	0.049	7	-
93/10/05	04:24	-109.0890	29.9400	4.33	0.038	5	-
93/10/11	07:19	-121.1727	36.5813	4.23	0.048	7	4.27
93/10/25	02:59	-119.7788	37.3198	2.71	-	1	-
93/10/26	09:24	-116.6520	34.9473	3.80	0.060	7	-
93/10/29	11:53	-118.1970	38.1630	4.01	0.018	5	3.95
93/11/10	14:54	-114.8450	44.4300	4.41	0.033	8	-
93/11/14	12:25	-120.4968	35.9523	4.75	0.045	7	4.81
93/11/28	08:21	-118.9355	37.6293	3.50	0.075	5	-
93/12/05	00:58	-102.7370	27.8310	4.85	0.027	6	-
93/12/20	17:37	-115.3590	32.3655	4.51	0.102	6	-
94/01/11	10:53	-121.7365	36.9872	4.24	0.023	6	4.13
94/01/17	12:30	-118.5370	34.2133	6.66	0.043	7	6.67
94/01/17	14:46	-122.4513	38.8012	4.31	0.035	6	-
94/02/03	09:05	-110.9760	42.7620	5.93	0.068	5	5.77
94/02/04	00:10	-116.9032	36.4860	3.97	0.079	5	4.00
94/03/15	18:58	-114.1210	29.2960	4.29	0.064	6	-
94/03/31	19:59	-120.3047	36.1835	4.40	0.033	7	4.38
94/04/07	18:32	-115.8910	31.6280	4.39	0.086	6	-
94/06/07	13:30	-114.0030	44.4930	5.13	0.042	7	5.04
94/06/11	19:28	-114.5060	30.0310	4.08	0.046	6	-
94/06/18	07:01	-121.2700	47.6210	4.21	0.071	2	-
94/06/26	08:42	-122.2890	37.9173	4.40	0.088	4	4.25
94/07/03	23:42	-118.2413	37.9290	3.78	0.059	5	3.61
94/08/08	21:17	-114.3730	30.5110	4.42	0.061	5	-
94/09/06	03:48	-112.3270	38.0780	4.37	0.094	5	-
94/09/12	12:23	-119.6520	38.8190	5.87	0.027	7	6.02
94/10/27	09:14	-109.6320	25.7040	5.09	0.047	6	5.05
94/11/17	20:29	-122.0440	42.3800	4.40	0.071	4	4.33
94/12/13	18:42	-114.3420	29.7540	4.53	0.119	5	-
94/12/27	18:53	-111.1230	25.7140	4.84	0.036	7	-
95/01/06	17:38	-113.8300	29.6850	4.57	0.061	5	-
95/01/28	06:26	-114.7770	44.4950	4.51	0.276	2	-
95/01/29	03:11	-122.3650	47.3880	5.04	0.028	2	5.05
95/01/29	16:02	-117.4080	31.6750	4.77	0.086	6	-
95/03/05	00:07	-118.8360	37.5970	4.43	0.029	6	4.14
95/03/26	14:32	-114.3510	31.2650	4.22	0.073	6	-
95/04/11	12:20	-115.4250	44.7940	4.11	0.134	2	-
95/04/14	00:32	-103.3250	30.2440	5.78	0.027	7	5.66
95/04/17	08:23	-112.2300	35.9660	4.13	0.066	6	-
95/05/02	19:31	-114.4570	48.1530	4.51	-	1	-
95/05/20	12:48	-121.9420	46.8810	3.96	-	1	-

Table 2 (continued). Network-averaged Coda M_w 's for the earthquakes examined, along with other event information. The coda- M_w σ 's are given along with the number of observations. For master events, the ground truth (GT) M_w 's are also provided.

Table 3: Aberrant WUS Catalog events					
Catalog	Longitude	Latitude	Date	Origin Time	Magnitude
WUS	-117.4945	37.3200	1990/12/13	01:01:01.5	4.30
SCSN	-117.2670	37.2500	"	01:01:00.0	2.70
UCB	-117.2670	37.2500	"	01:01:00.0	3.00
UNR	-117.3500	37.3615	"	01:00:59.7	2.83
WUS	-118.9355	37.6293	1993/11/28	08:21:23.0	5.10
SCSN	-118.9352	37.6380	"	08:21:22.9	2.50
UNR	-118.9410	37.6287	"	08:21:22.7	1.55
WUS	-119.8458	38.7733	1994/01/16	16:59:33.6	4.80
UNR	-119.7690	38.8105	"	16:59:32.3	1.36
WUS	-120.2617	36.1683	1991/09/15	17:34:35.6	4.00
SCSN	-120.216	36.2150	"	17:34:36.3	2.40
WUS	-122.0000	42.7170	1993/09/21	03:36:00.5	4.20
WUS	-119.7788	37.3198	1993/10/25	02:59:06.1	4.70

Table 3. Aberrant events from the WUS NEHRP catalog. Each set of rows within a single box are for one particular event. The bottom two events listed have no compatible events in terms of location and origin-time in the appropriate regional seismic bulletins, *i. e.* they are non-existent events.

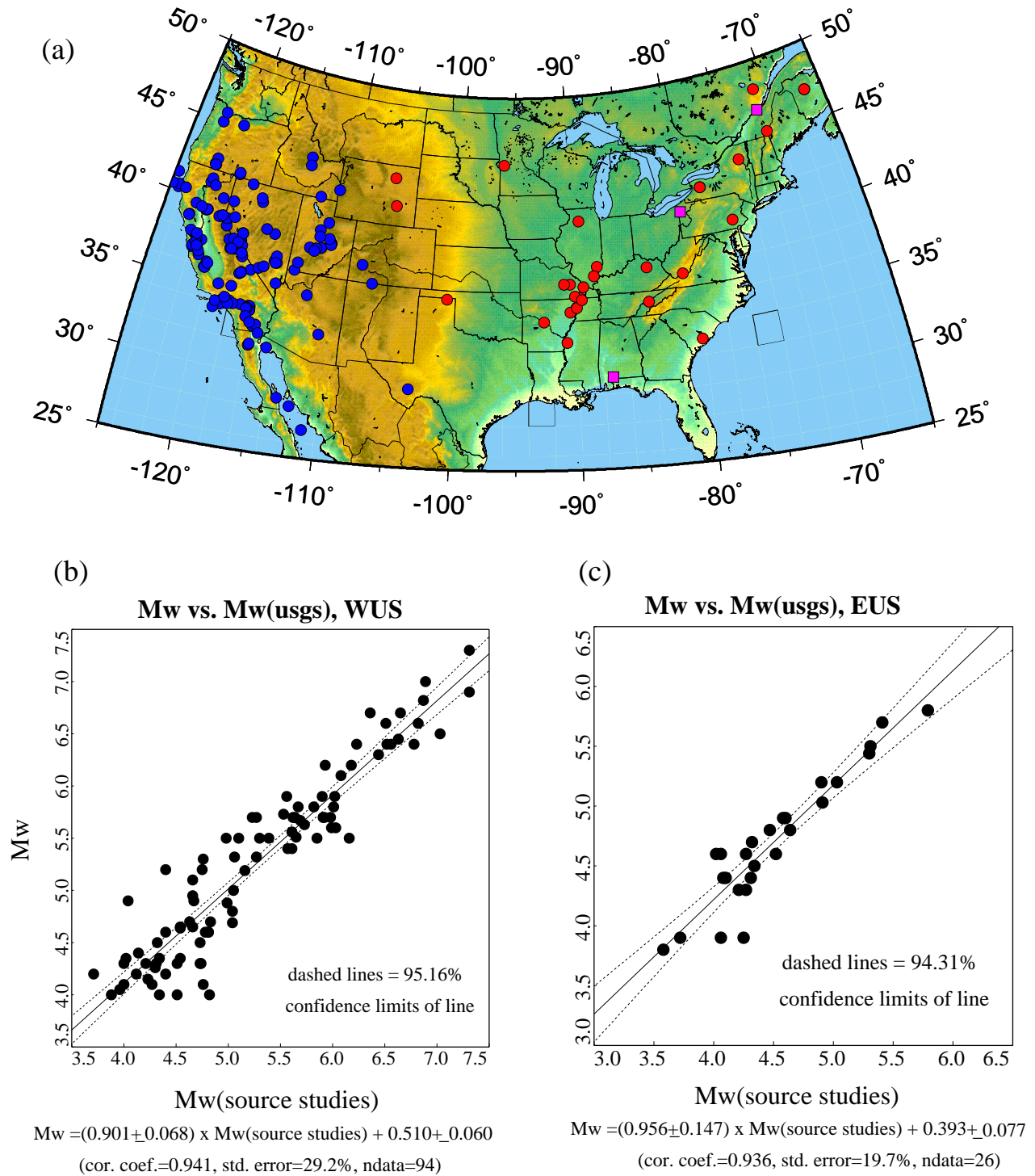


Figure 1. (a) Map of the continental United States with earthquakes from the the current seismic-hazard-mapping moment magnitude catalog (blue circles indicate WUS catalog events, red circles EUS catalog events, and pink boxes are for more recent significant eastern earthquakes) for which seismic moment has been directly measured. (b) Linear regression results for M_w 's from the WUS catalog vs. M_w compiled from various published source studies and catalogs, and (c) analogous results for the CEUS catalog.

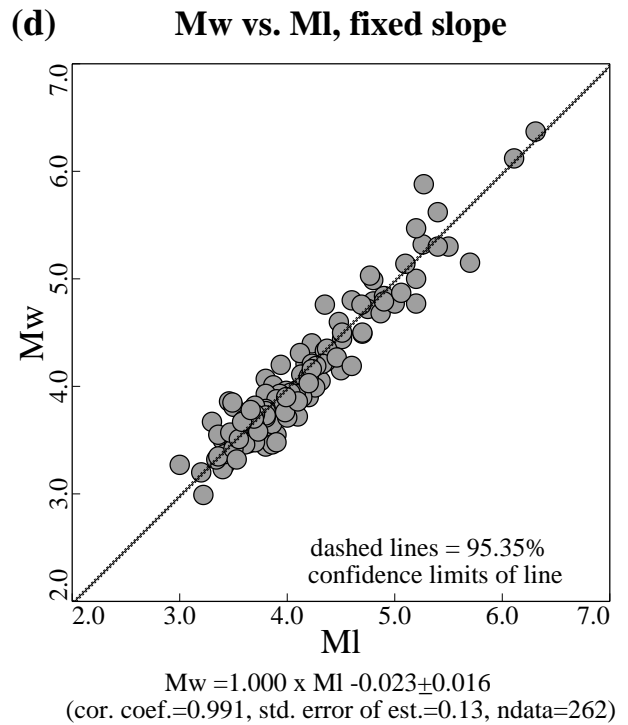
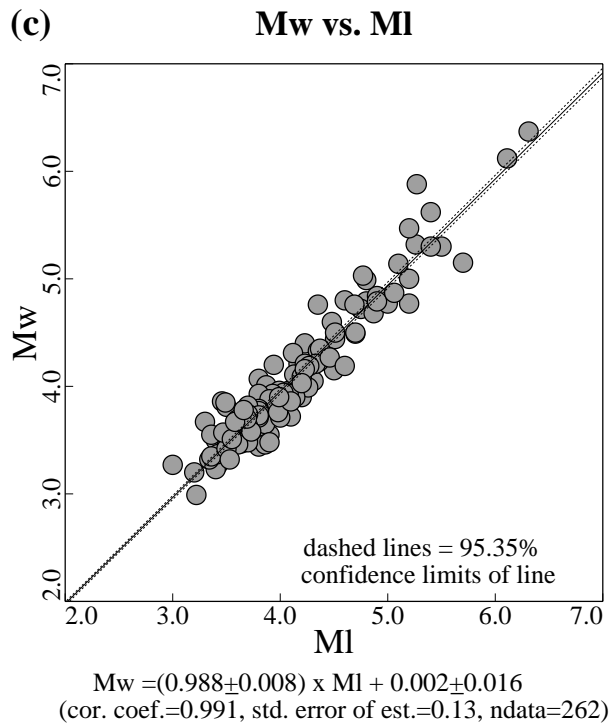
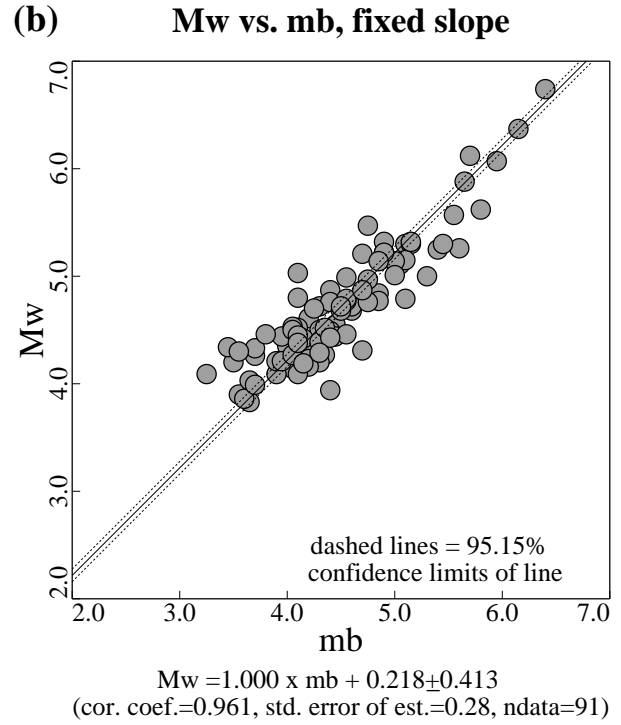
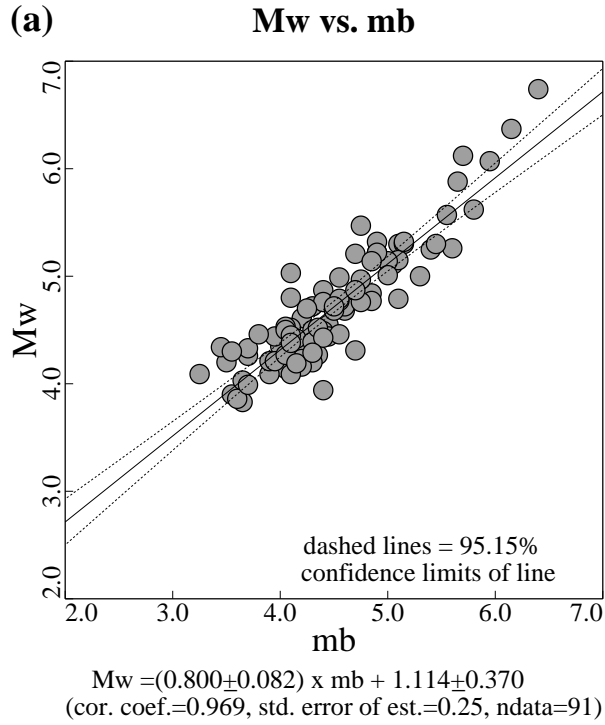


Figure 2. Regression results M_w vs. (a) m_b , (b) m_b assuming a fixed slope, (c) M_L and (d) M_L assuming a fixed slope.

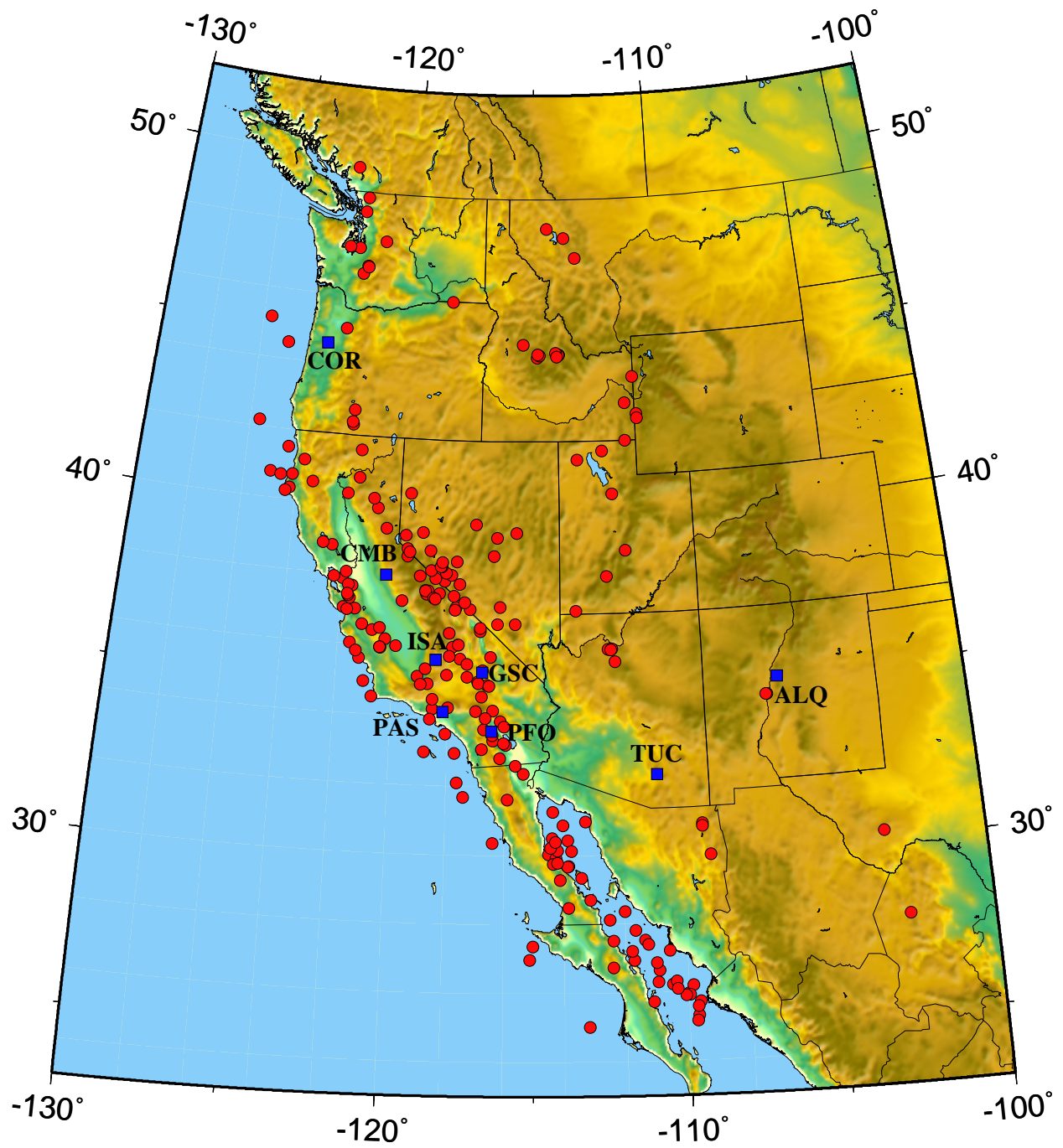


Figure 3. Map of western United States and bordering regions, with the earthquakes (red circles) and seismic stations (blue squares) used in this study.

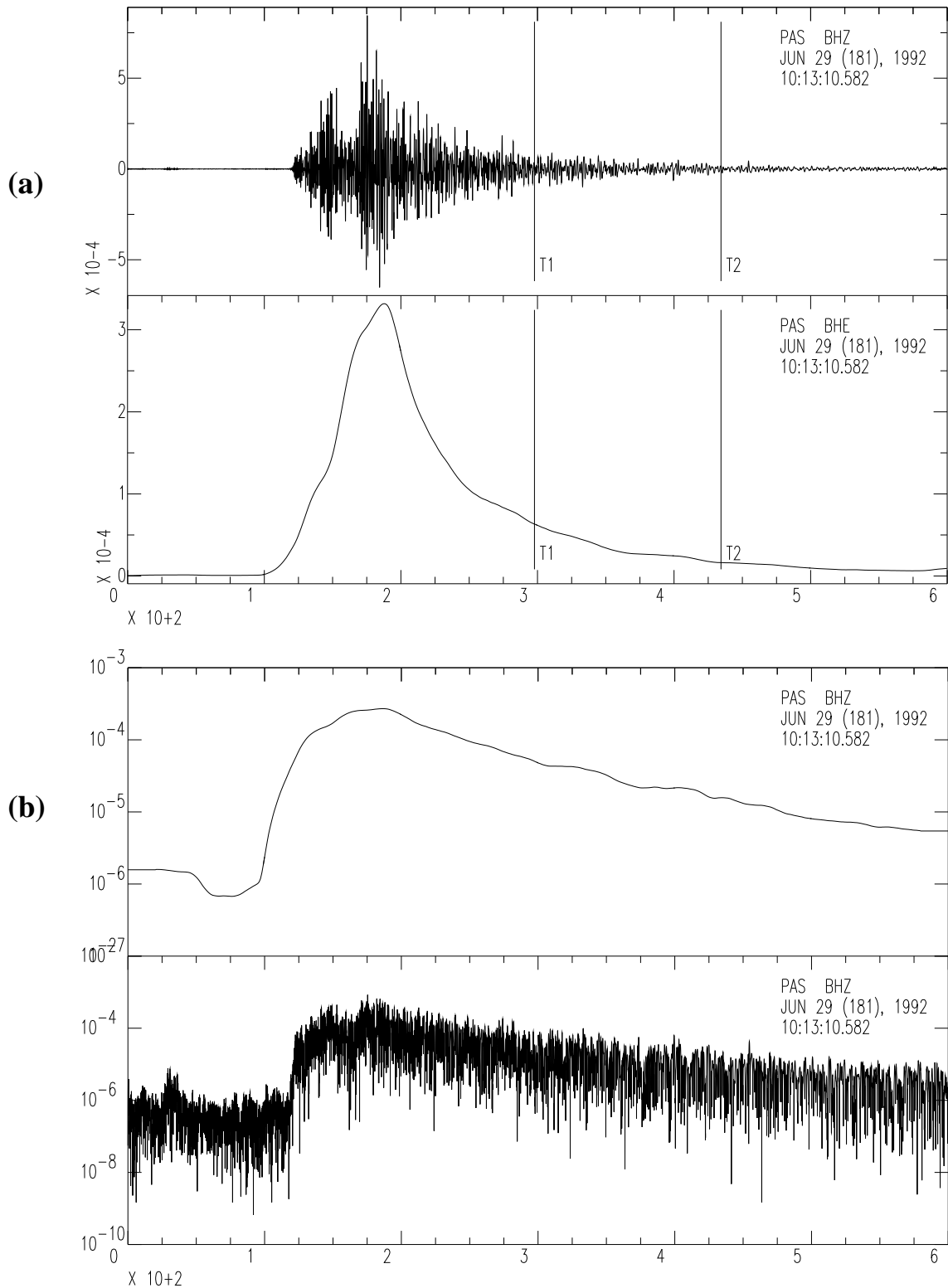
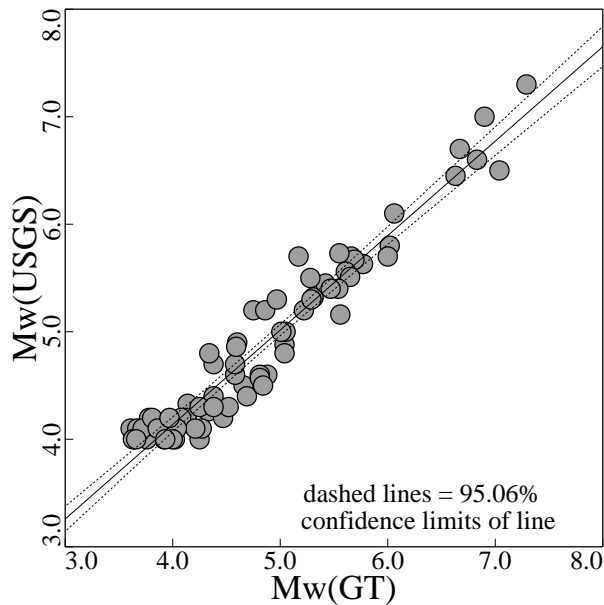


Figure 4. (a) Example WWSP-convolved displacement waveform (top) and the corresponding smoothed envelope (bottom); T1 and T2 denote the portion of the time window of the time series over which the coda amplitude and duration are measured. (b) Example comparison of log amplitude of the envelope to the displacement.

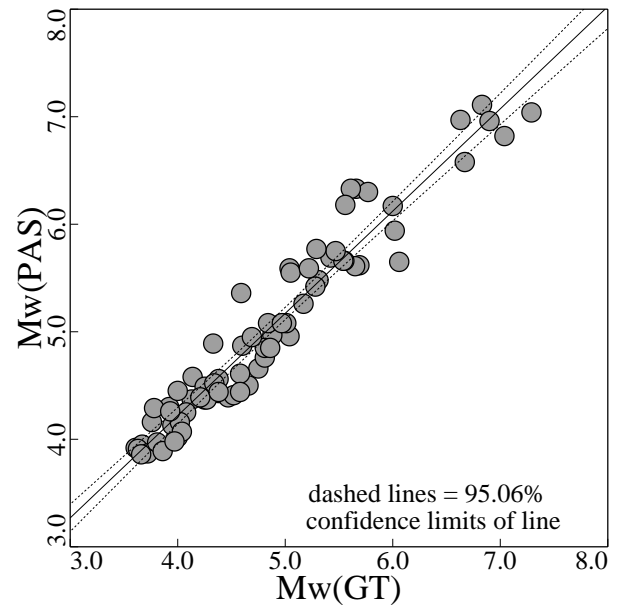
(a) Mw(GT) vs. Mw(USGS)



$$Mw(USGS) = (0.879 \pm 0.056) \times Mw(GT) + 0.624 \pm 0.272$$

(cor. coef.=0.977, std. error of est.=0.21, ndata=72)

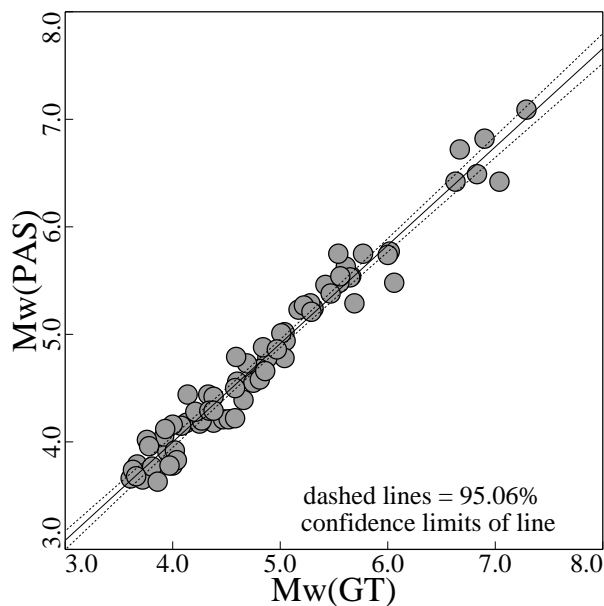
(b) Mw(GT) vs. Mw(PAS), dur.



$$Mw(PAS) = (0.951 \pm 0.061) \times Mw(GT) + 0.416 \pm 0.296$$

(cor. coef.=0.972, std. error of est.=0.23, ndata=72)

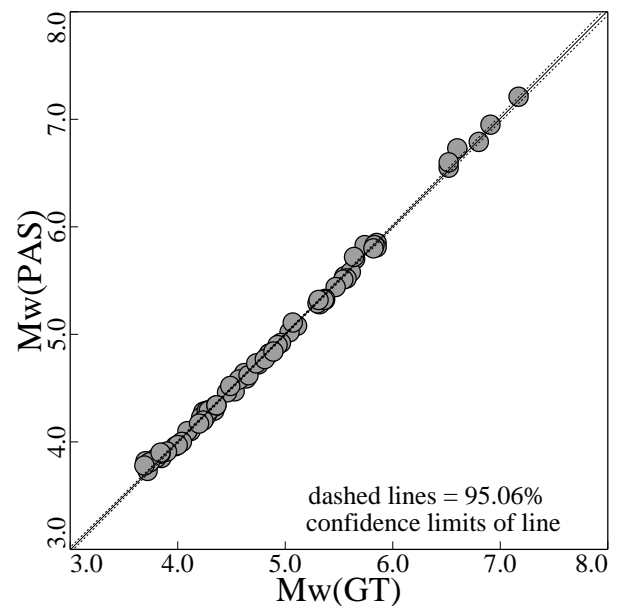
(c) Mw(GT) vs. Mw(PAS), dist.



$$Mw(PAS) = (0.915 \pm 0.042) \times Mw(GT) + 0.340 \pm 0.202$$

(cor. coef.=0.987, std. error of est.=0.16, ndata=72)

(d) Mw(GT) vs. Mw(PAS), 4-var

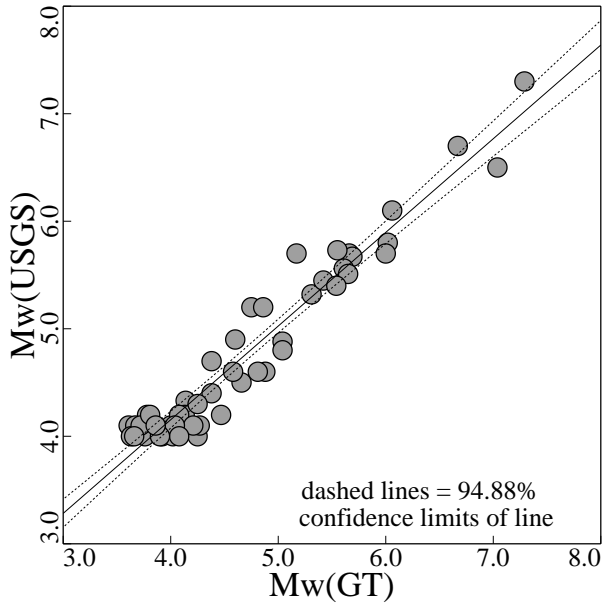


$$Mw(PAS) = (1.003 \pm 0.012) \times Mw(GT) - 0.015 \pm 0.058$$

(cor. coef.=0.999, std. error of est.=0.04, ndata=72)

Figure 5. Regression results of ground-truth (GT) moment magnitudes (M_w) vs. (a) USGS NEHRP catalog M_w 's, (b) coda magnitude, measured at station PAS, using 3-variable error minimization which includes a linear duration term, (c) coda magnitude using 3-variable error minimization which includes a linear distance term, and (d) the final 4-variable error minimization coda magnitude measured at PAS.

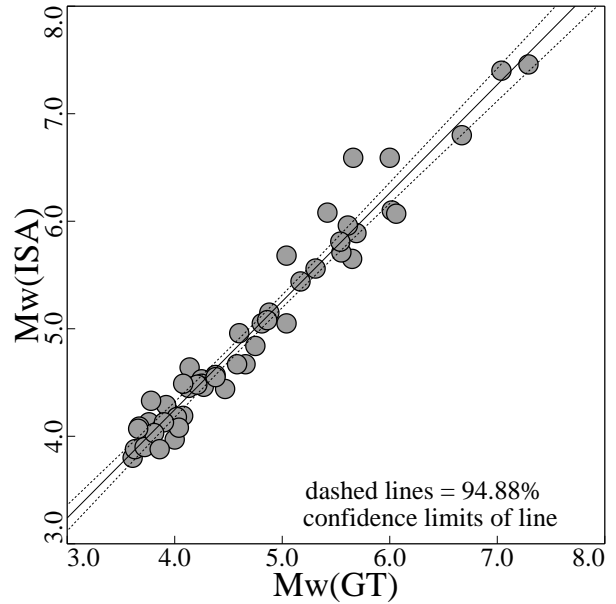
(e) Mw(GT) vs. Mw(USGS)



$$Mw(USGS) = (0.871 \pm 0.066) \times Mw(GT) + 0.671 \pm 0.310$$

(cor. coef.=0.977, std. error of est.=0.21, ndata=50)

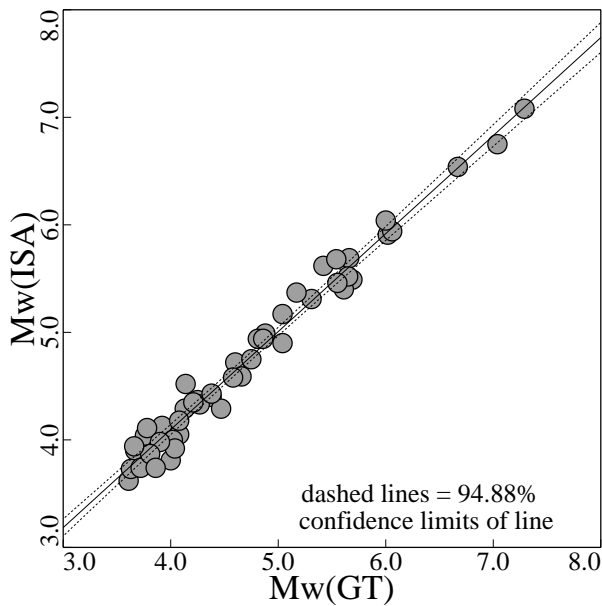
(f) Mw(GT) vs. Mw(ISA), dur.



$$Mw(ISA) = (1.007 \pm 0.060) \times Mw(GT) + 0.218 \pm 0.285$$

(cor. coef.=0.981, std. error of est.=0.20, ndata=50)

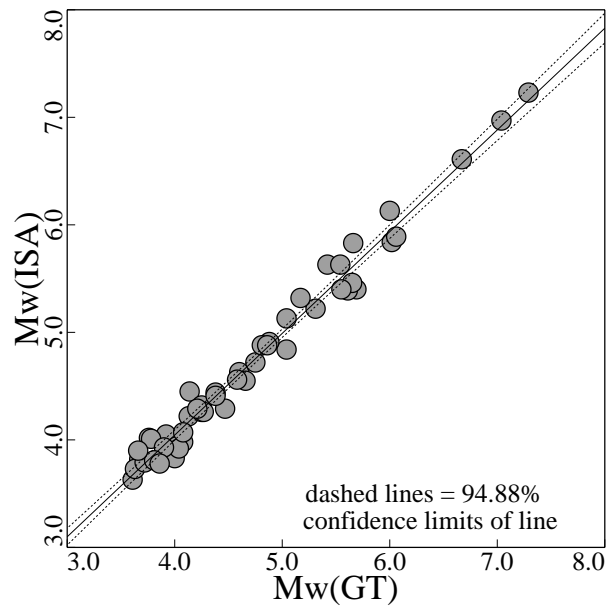
(g) Mw(GT) vs. Mw(ISA), dist.



$$Mw(ISA) = (0.911 \pm 0.040) \times Mw(GT) + 0.451 \pm 0.189$$

(cor. coef.=0.991, std. error of est.=0.13, ndata=50)

(h) Mw(GT) vs. Mw(ISA), 4-var



$$Mw(ISA) = (0.946 \pm 0.040) \times Mw(GT) + 0.261 \pm 0.187$$

(cor. coef.=0.992, std. error of est.=0.13, ndata=50)

Figure 5 (continued). M_w regression results for events recorded at ISA. Ground-truth (GT) moment magnitudes (M_w) vs. (e) USGS NEHRP catalog M_w 's, (f) coda magnitude, measured at station ISA, using 3-variable error minimization which includes a linear duration term, (g) coda magnitude using 3-variable error minimization which includes a linear distance term, and (h) the final 4-variable error minimization coda magnitude measured at PAS.

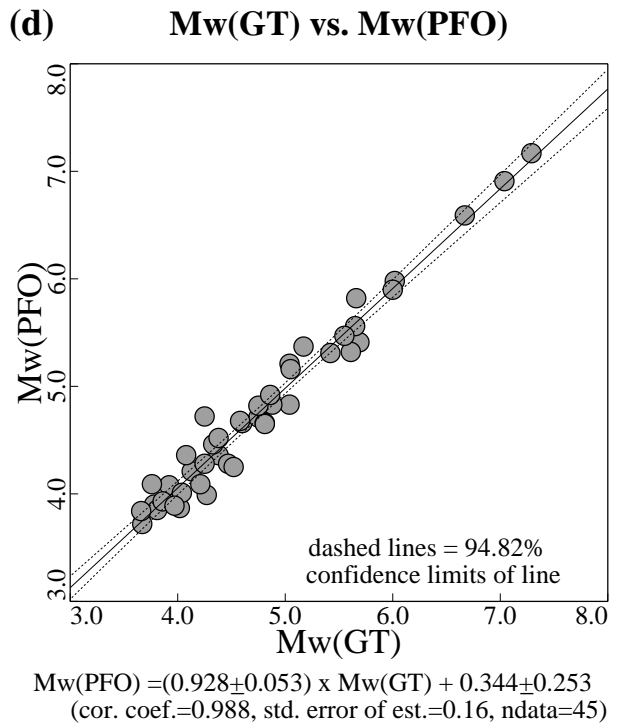
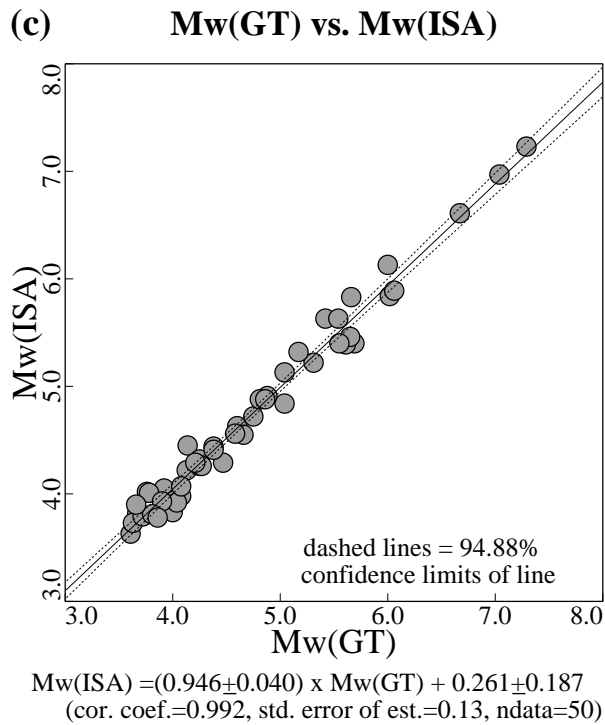
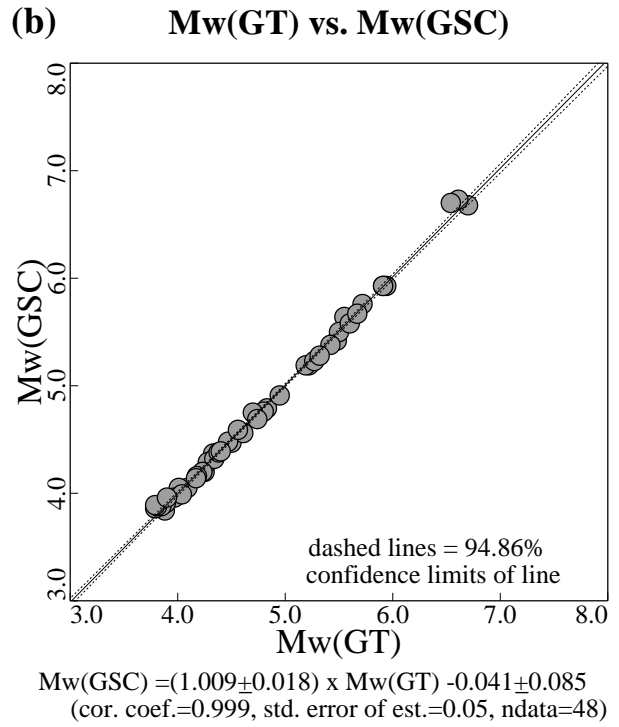
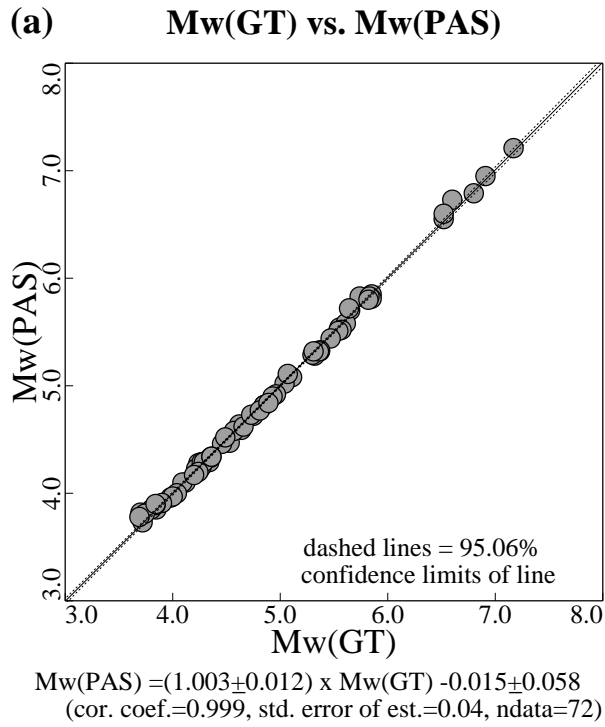
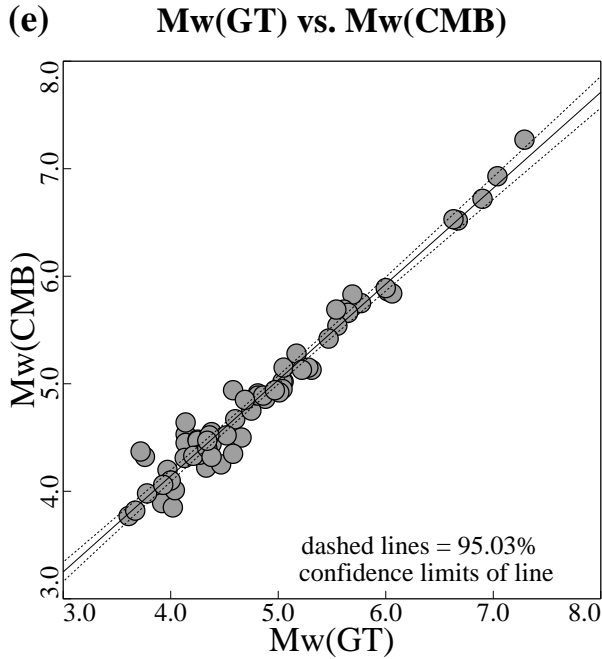
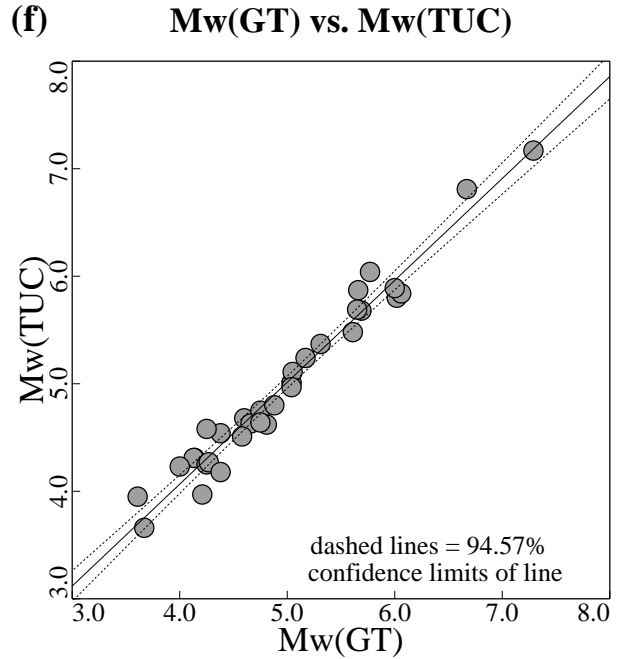


Figure 6. Regression results for final single-station coda M_w 's versus GT values for the stations PAS (a), GSC (b), ISA (c) and PFO (d).



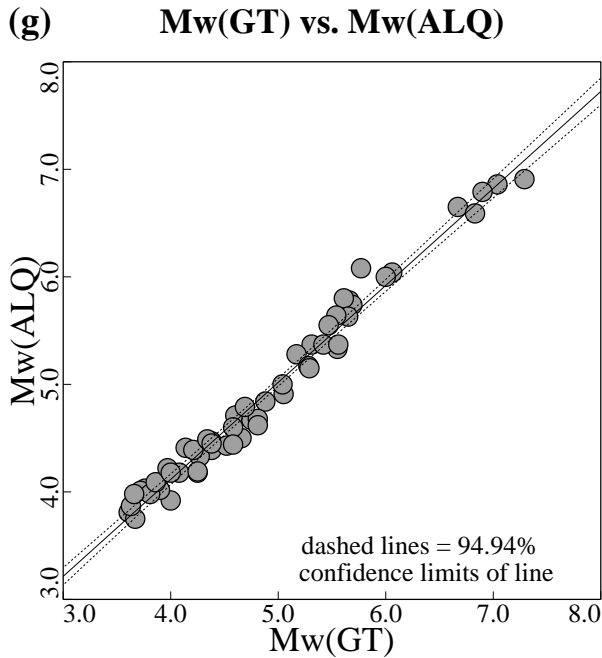
$$Mw(CMB) = (0.892 \pm 0.044) \times Mw(GT) + 0.574 \pm 0.212$$

(cor. coef.=0.988, std. error of est.=0.15, ndata=67)



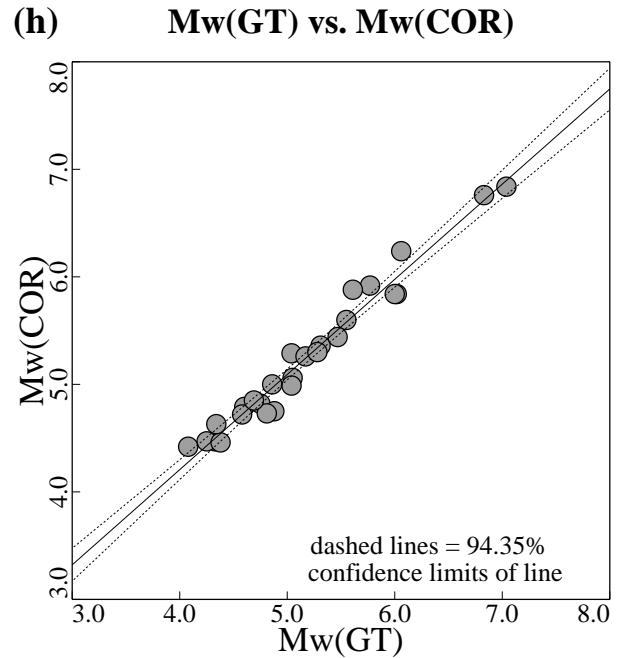
$$Mw(TUC) = (0.948 \pm 0.064) \times Mw(GT) + 0.275 \pm 0.320$$

(cor. coef.=0.988, std. error of est.=0.16, ndata=33)



$$Mw(ALQ) = (0.902 \pm 0.038) \times Mw(GT) + 0.509 \pm 0.184$$

(cor. coef.=0.991, std. error of est.=0.13, ndata=55)

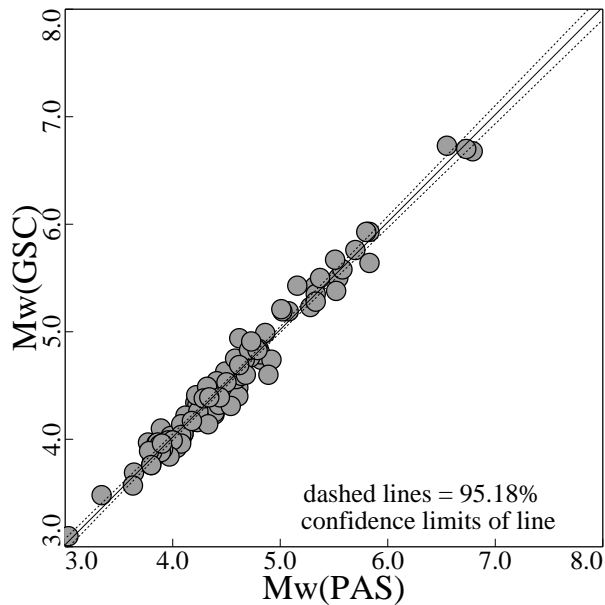


$$Mw(COR) = (0.885 \pm 0.064) \times Mw(GT) + 0.667 \pm 0.332$$

(cor. coef.=0.992, std. error of est.=0.12, ndata=27)

Figure 6 (continued). Regression results for final single-station coda M_w 's versus GT values for the stations CMB (e), TUC (f), ALQ (g) and COR (h).

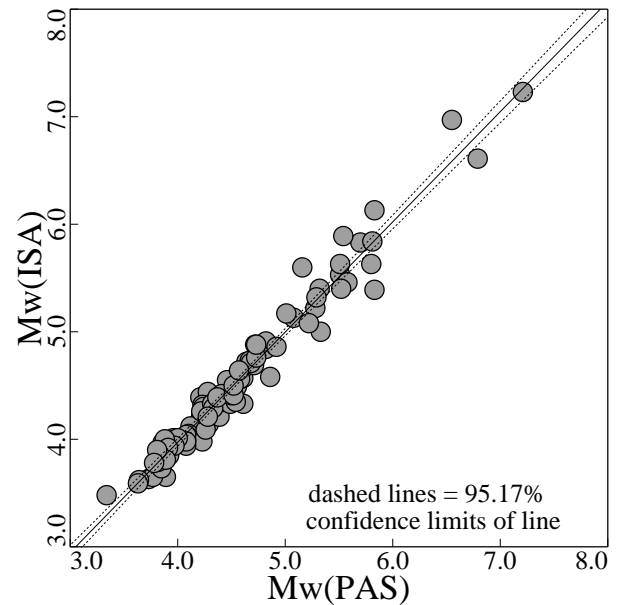
(a) Mw(PAS) vs. Mw(GSC)



$$Mw(GSC) = (1.000 \pm 0.033) \times Mw(PAS) + 0.021 \pm 0.149$$

(cor. coef.=0.993, std. error of est.=0.11, ndata=101)

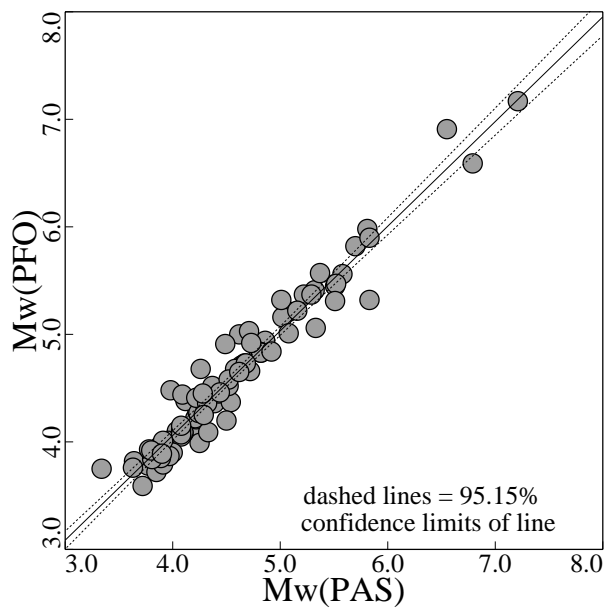
(b) Mw(PAS) vs. Mw(ISA)



$$Mw(ISA) = (1.025 \pm 0.040) \times Mw(PAS) - 0.127 \pm 0.180$$

(cor. coef.=0.990, std. error of est.=0.14, ndata=99)

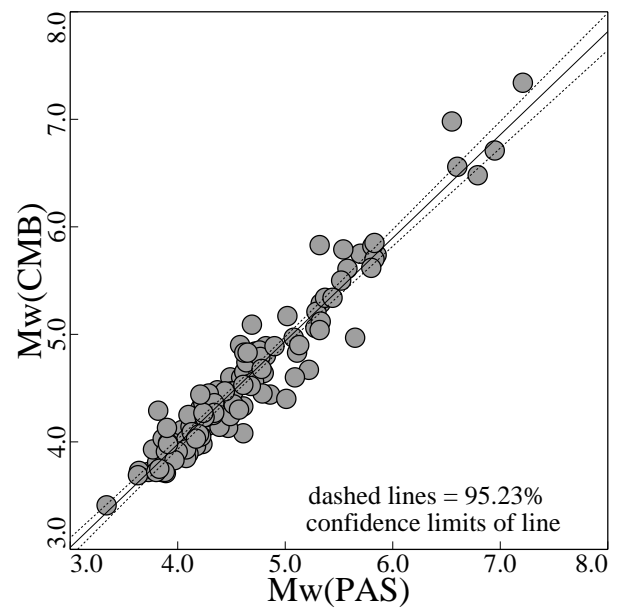
(c) Mw(PAS) vs. Mw(PFO)



$$Mw(PFO) = (0.973 \pm 0.049) \times Mw(PAS) + 0.167 \pm 0.222$$

(cor. coef.=0.986, std. error of est.=0.16, ndata=93)

(d) Mw(PAS) vs. Mw(CMB)



$$Mw(CMB) = (0.959 \pm 0.050) \times Mw(PAS) + 0.141 \pm 0.230$$

(cor. coef.=0.980, std. error of est.=0.20, ndata=124)

Figure 7. Inter-station coda M_w regression results between PAS and GSC (a), ISA (b), PFO (c) and CMB (d).

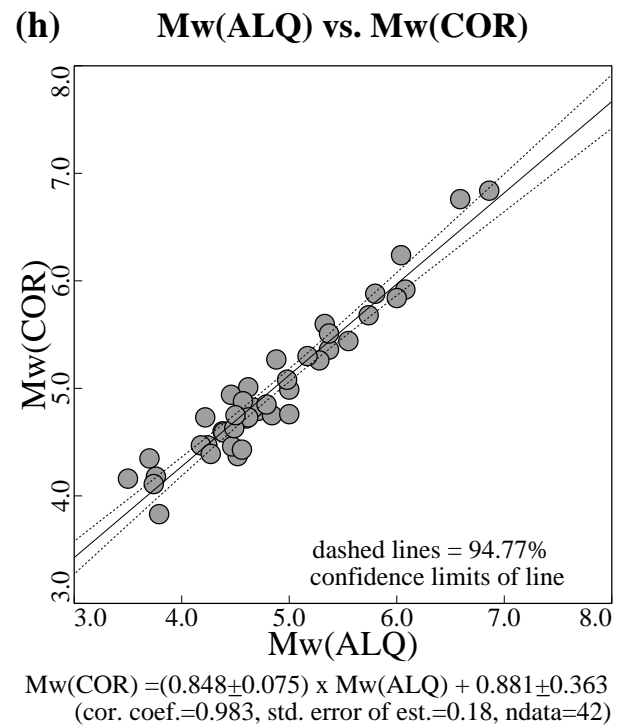
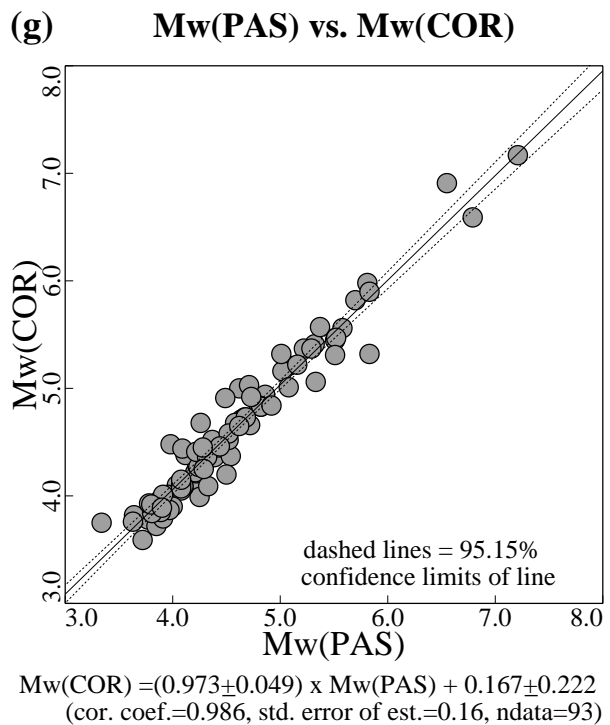
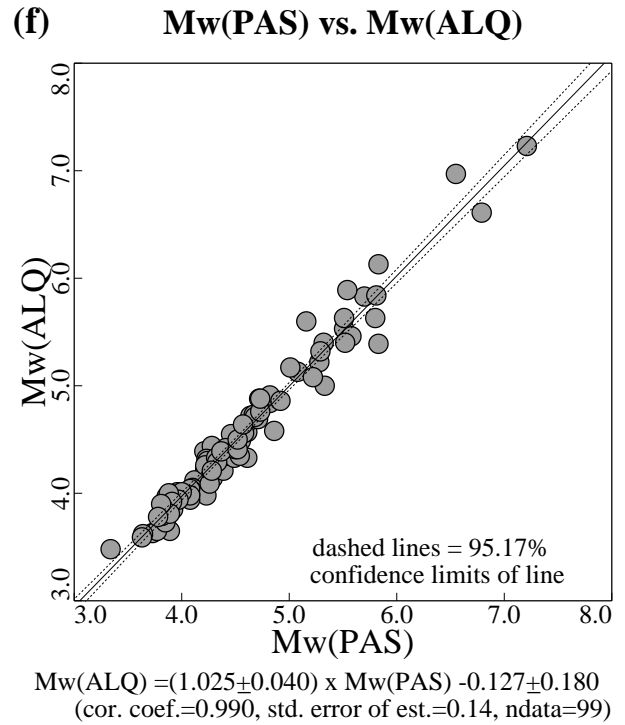
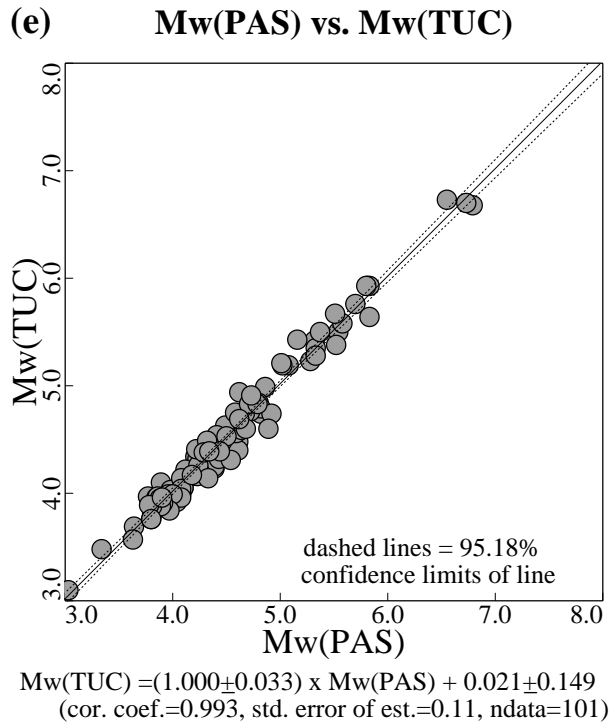
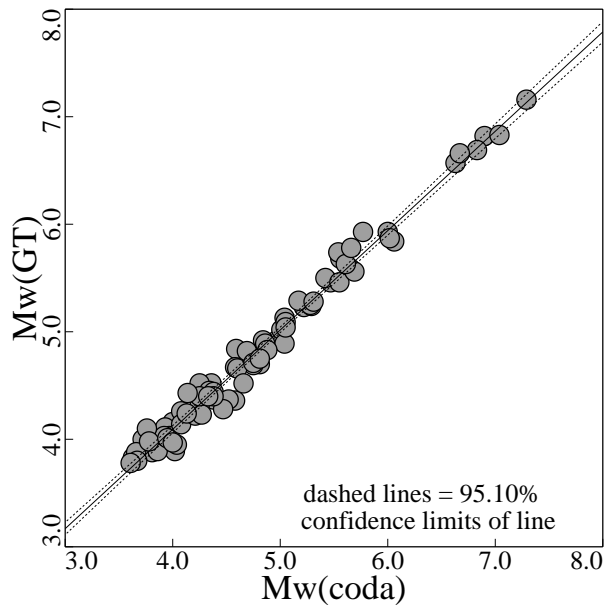


Figure 7 (continued). Inter-station coda M_w regression results between PAS and TUC (e), ALQ (f), COR (g), and between ALQ and COR (h)

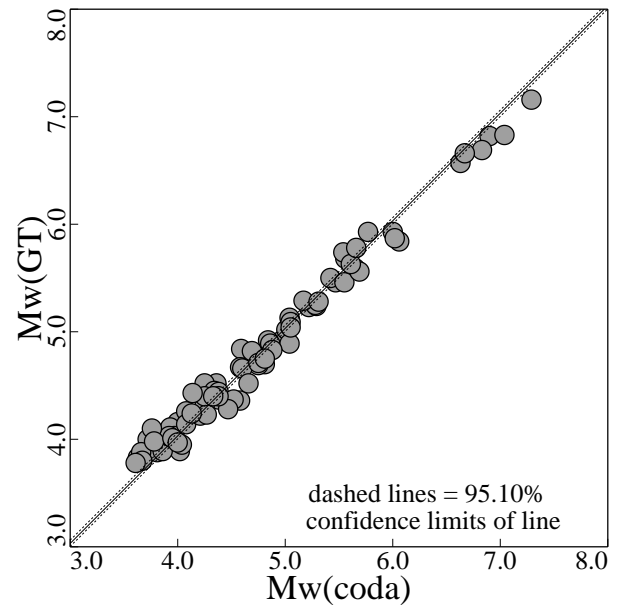
(a) Mw(coda) vs. Mw(GT)



$$Mw(GT) = (0.924 \pm 0.028) \times Mw(coda) + 0.398 \pm 0.136$$

(cor. coef.=0.994, std. error of est.=0.11, ndata=79)

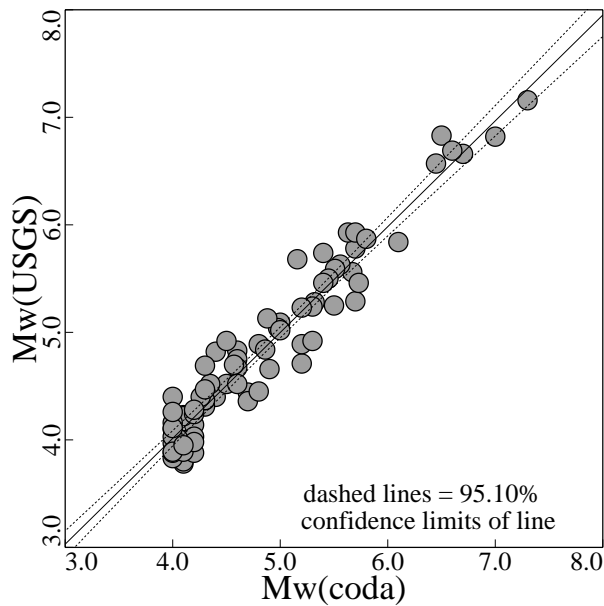
(b) Mw(coda) vs. Mw(GT), fixed slope



$$Mw(GT) = 1.000 \times Mw(coda) + 0.033 \pm 0.159$$

(cor. coef.=0.992, std. error of est.=0.13, ndata=79)

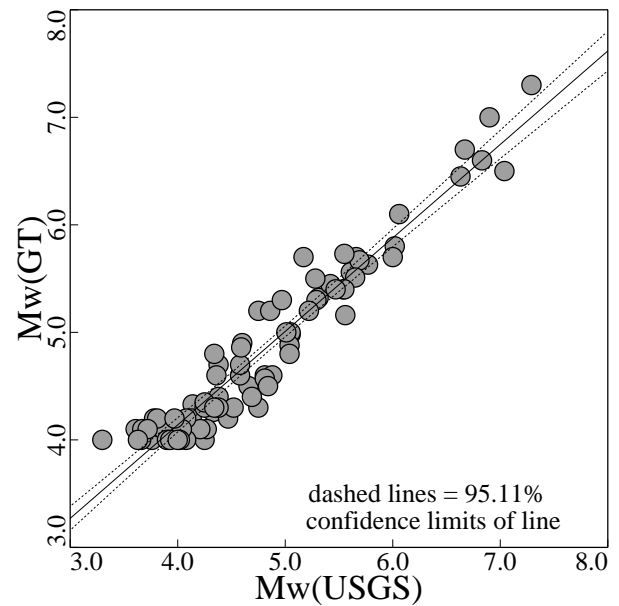
(c) Mw(coda) vs. Mw(USGS)



$$Mw(USGS) = (0.984 \pm 0.061) \times Mw(coda) + 0.079 \pm 0.293$$

(cor. coef.=0.976, std. error of est.=0.22, ndata=79)

(d) Mw(USGS) vs. Mw(GT)



$$Mw(GT) = (0.869 \pm 0.055) \times Mw(USGS) + 0.663 \pm 0.263$$

(cor. coef.=0.976, std. error of est.=0.22, ndata=81)

Figure 8. Regression results of network-averaged coda M_w vs. (a) ground-truth (GT) M_w , (b) ground-truth M_w assuming a constrained slope of unity, and (c) USGS NEHRP catalog M_w , as well as (d) USGS M_w vs. ground-truth M_w .

Bibliography of Project-Related Publications and Presentations

Woods, B. B., 2000. Revising Catalog Moment Magnitudes for Western U. S. earthquakes using coda measurements, *EOS. Trans. AGU*, **81**(48), Fall Meeting Suppl., Abstract S61A-26.

Woods, B. B., 2002. A New Method of Determining Coda Magnitude and Its Application to Earthquakes in the Western U. S., *submitted to Bull. Seism. Soc. Am.* (A redacted version of this report).

Non-technical Summary for:

**REVISING MOMENT-MAGNITUDE EARTHQUAKE CATALOGS FOR
USE IN GENERATING THE NATIONAL SEISMIC HAZARD MAPS**

The current earthquake catalogs used to generate the National Seismic Hazard Maps (NSHM) rely on earthquake moment magnitudes based on conversions of other magnitude scales which do not necessarily well characterize the long-period source character of earthquakes, necessary to predict/estimate ground motions of future earthquakes. The purpose of this work is to revise these moment-magnitude (M_w) catalogs for the period 1988 to 1995 by directly measuring seismic moment from short-period coda waves. This type of magnitude measurement gives robust, accurate estimates of earthquake size, necessary for realistically estimating earthquake hazards.